Journal of Materials Chemistry B

Accepted Manuscript

ROYAL SOCIETY OF CHEMISTRY

www.rsc.org/materialsB

Journal Name

Journal of Materials Chemistry B

Dynamic Article Links ►

Cite this: DOI: 10.1039/c0xx00000x

www.rsc.org/xxxxxx

ARTICLE TYPE

Protein-directed approaches to functional nanomaterials: a case study of lysozyme

Yubin Ding,[a] Leilei Shi,[a] and Hui Wei*[a]

Received (in XXX, XXX) Xth XXXXXXXXX 20XX, Accepted Xth XXXXXXXXX 20XX

DOI: 10.1039/b000000x

Functional nanomaterials have found wide applications in diverse areas due to their intrinsically different properties compared with bulk materials. To achieve the goal of preparing functional nanomaterials, various strategies have been successfully developed. Among them, biomolecules-directed approach has been extensively explored to synthesize a lot of functional nanomaterials owing to their programmability, self-assembly and recognition capabilities. This Feature Article highlights the use of lysozyme as a model protein to direct synthesis of nanomaterials. Future advances in rational *de novo* design and synthesis of functional nanomaterials with proteins will depend on a deep understanding of the synthetic strategies and the formation mechanisms. This Feature Article discusses the synthesis of nanomaterials with lysozyme in both solution phase and crystal form. The synthetic strategies, formation mechanisms and wide applications of several kinds of materials, such as metal, oxide, metal sulfides, and composites, are covered. The lessons from this case study will provide invaluable guidance in future materials design using protein and other biomolecules. Rational design of personalized functional nanomaterials will be possible in future (366 references).

1. Introduction

Functional nanomaterials have found wide applications in various areas, from catalysis, energy conversion and storage, information science, to environmental and biomedical science, due to their intrinsically unique properties compared with bulk materials.[1-93] To achieve the goal of synthesizing functional nanomaterials, numerous innovative approaches have been successfully developed. Among them, biomolecules-directed approach has been extensively explored to prepare a variety of functional nanomaterials owing to their programmability, self-assembly and recognition capabilities.[94-153] In particular, proteins provide several distinct characteristics for nanomaterials fabrications, including their nanoscaled sizes, distinctive molecular structures, diverse functionalities, highly-specific biorecognition, and various self-assembly abilities. Further, proteins with designed structures and functions can be obtained through protein engineering. More, atomic resolution structural information can be provided via protein crystallography, allowing for mechanism studies. It has been demonstrated that proteins, in the forms of monomers, assemblies, and even single crystals, can direct the formation of many functional materials, such as metal nanoclusters, metal nanoparticles, metal oxides, silica, semiconductor quantum dots, conducting polymers and reduced graphene oxide, etc.[108-121, 154-166] Despite significant advances, the rational design and preparation of functional nanomaterials with intentionally desired properties remains great challenges in the field due to the lack of full understanding of the nanomaterials formation mechanism and protein-nanomaterials interactions.[159]

To address these challenges and highlight the significant progresses in the field, this feature article discusses the uses of lysozyme as a model protein to prepare various nanomaterials, to elucidate the growth mechanism and protein-nanomaterials interactions, and to demonstrate the key applications (note: lysozyme used throughout this paper is from chicken egg white unless otherwise specified) (Figure 1). Unlike other model proteins, such as bovine serum albumin, ferritin and caged virus proteins, lysozyme is a relative small protein with 129 amino acid residues and a calculated molecular weight of 14307 Da,[167] which makes it easier access to characterization and manipulation. Lysozyme has 8 cysteine residues, forming 4 disulfide bonds, and 1 surface-exposed histidine residue (Figure S1). Lysozyme is also relatively easy to be crystallized, allowing for obtaining atomic resolution insights into structure information.[159, 162, 168] Further, lysozyme is an enzyme, which enables us to investigate its biological activity after forming nanomaterials and to prepare multifunctional materials (Figure S2). In addition, lysozyme is stable over wide temperature and pH ranges, making it suitable for varieties of synthetic approaches. In this article, both lysozyme in solution phase-directed approach and lysozyme crystal-directed approach to functional nanomaterials are summarized. First, the synthesis and careful characterization of metal nanoclusters (such as gold, silver, copper, platinum, and bimetallic nanoclusters) in solution phase are discussed. The possible growth mechanisms are also explored with the aid of detailed kinetic and mass spectroscopic studies, etc. Besides applications in sensing and tumour cells detection, biological activity study of lysozyme after forming nanoclusters is also

covered. Then, the studies of large metal nanoparticles and other materials in solution phase are summarized. Their formation mechanism, antimicrobial activity, assembly and numerous applications are investigated. In Section 3, the use of lysozyme crystals (both cross-linked crystals and intact single crystals) to direct synthesis of different kinds of hybrid nanomaterials, from plasmonic metal nanomaterials and fluorescent quantum dots to magnetic nanoparticles and conducting polymers, is discussed. The growth mechanisms and structure evolution are elucidated with combination of electron microscopy with tomography, X-ray crystallography, and other techniques. The development of effective methods to tune the nanomaterials' properties, such as optical and magnetic properties, is presented. Several interesting applications, including plasmonic and catalytic applications, are also described. Finally, the current challenges, opportunities and perspectives in rational materials design using lysozyme and other proteins are discussed.

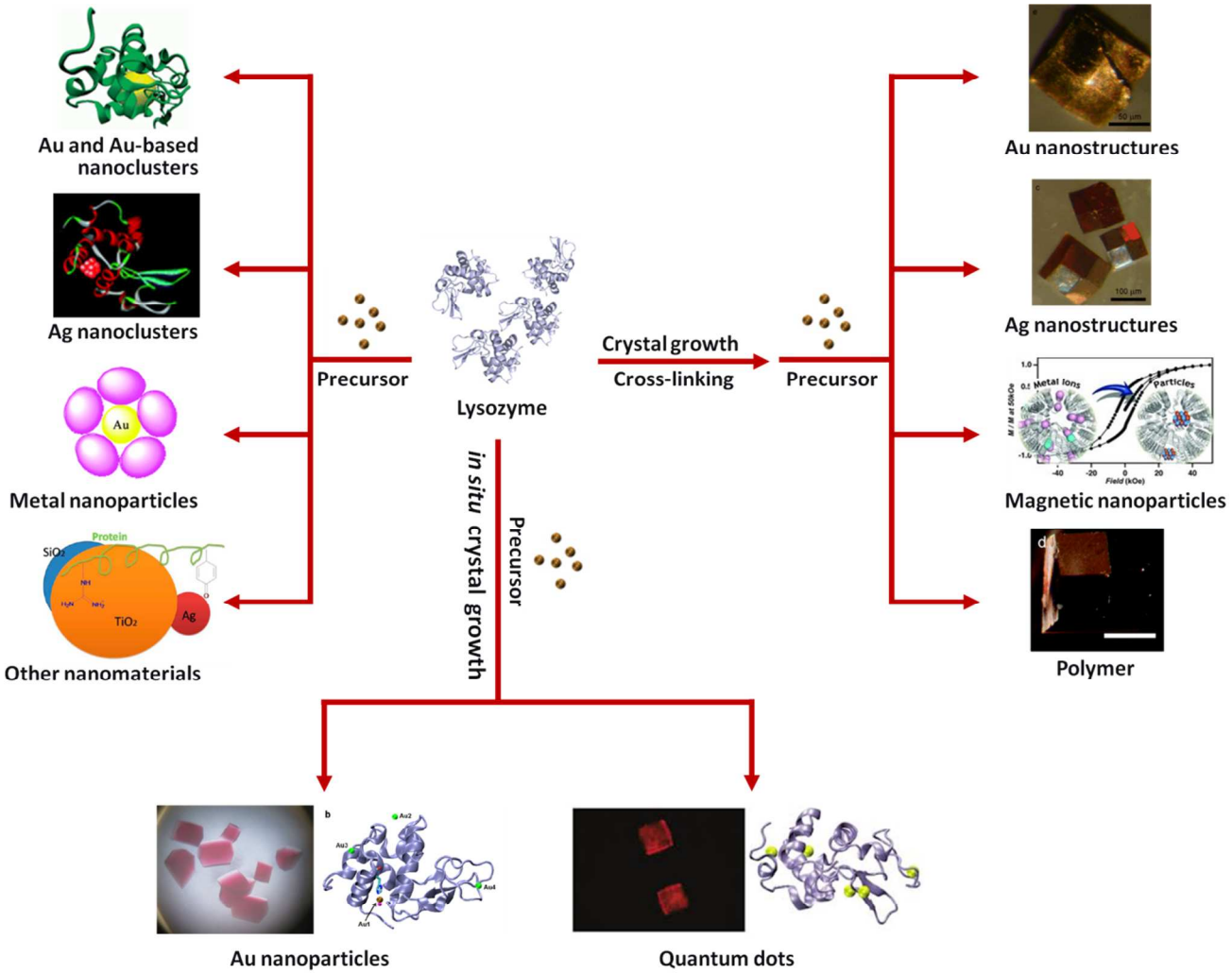

Figure 1. Lysozyme-directed approaches to functional nanomaterials. (left) solution phase-directed approach, (right) cross-linked crystal-directed approach, and (bottom) intact single crystal-directed approach to functional nanomaterials. From upper right to upper left (clockwise): reprinted with permission from ref.[114], copyright (2010) John Wiley and Sons; ref.[169], copyright (2012) John Wiley and Sons; ref.[164], copyright (2012) Royal Society of Chemistry; ref.[162], copyright (2013) Tsinghua University Press and Springer; ref.[159], copyright (2011) Nature Publishing Group; ref.[170], copyright (2013) American Chemical Society; ref.[171], copyright (2007) American Chemical Society; ref.[172], copyright (2012) Royal Society of Chemistry; ref.[155], copyright (2010) Royal Society of Chemistry.

Readers are referred to numerous excellent reviews for more comprehensive information regarding synthesis of functional nanomaterials with other proteins and biomolecules rather than lysozyme (note: due to the limited space, only a small number of reviews are cited in the references).[173-191] Under certain conditions, lysozyme itself can also form innovative functional materials and be engineered for diverse exciting applications.[192-196] Using target proteins (such as lysozyme) as the template, molecularly imprinted polymers have been successfully *in situ* coated onto supporting nanoparticles (e.g., magnetic or silica nanoparticles) to construct core-shell structured functional materials for selective recognition and enrichment of target proteins.[197-204] However, these topics are out of the scope of the current review and will not be covered.

2. Lysozyme in solution phase

In this section, the use of lysozyme to direct formation of

functional nanomaterials in solution phase is discussed.

2.1 Metal nanoclusters

Metal nanoclusters, consisting of a few to several hundred metal atoms and having a size smaller than 2 nm, have received considerable attention because of their ultrasmall and atomically precise size, nontoxicity, and unique physical, electrical, electrochemical, catalytic, and optical properties.[156, 184, 205-289] They have already found wide applications in many areas such as bioconjugation, catalysis, nanodevices, bioimaging, biosensing, and cancer therapy, etc. Researchers have established that proteins, including lysozyme, can direct the formation of metal nanoclusters.[113, 116, 117, 120, 146, 154, 155, 234, 290-304] Compared with other methods so far developed, the protein-directed approach can produce metal nanoclusters with good water solubility, high stability, strong fluorescence, biocompatibility and biofunctionality, etc. The method is also environmentally friendly and the nanoclusters formed are ready for further bioconjugation. Several kinds of metal nanoclusters, including Au, Ag, Cu, Pt, and bimetallic nanoclusters, have been synthesized via lysozyme-directed approaches.[121, 155, 172, 299, 305-313]

2.1.1 Au

Synthetic protocols. Previous work showed that fluorescent Au nanoclusters could be formed under basic condition using bovine serum albumin (BSA) as both reducing agent and capping ligand.[154] It suggested that metal ions could be reduced by tyrosine (and/or tryptophan) residues through the phenolic groups. Inspired by this interesting discovery, Wei and co-workers demonstrated that highly fluorescent Au nanoclusters could be synthesized in basic aqueous solution by using lysozyme as reducing and stabilizing agent for the first time (Figure 2A).[155] The Au nanoclusters were formed after incubation of the mixture of $HAuCl_4$ and lysozyme at 37 °C under basic condition due to the reduction of $HAuCl_4$ by tyrosine (and/or tryptophan) residues of lysozyme. The optimal synthetic approach could be obtained by optimizing the molar ratios of lysozyme to $HAuCl_4$, the concentrations of lysozyme, $HAuCl_4$ and NaOH, the reaction time and incubation temperature, etc. Molar ratios of 0.17:1 and 0.18:1 of lysozyme to $HAuCl_4$ were used by Wei et al. and Xu et al., respectively.[155, 310] Higher molar ratios were also employed by others.[306, 309] Most of the reports adopted Wei's approach to prepare lysozyme stabilized Au nanoclusters.[121, 306-309, 312] Chen's group showed that the reaction time could be significantly shortened from several hours to less than 1 hour by using microwave heating instead of 37 °C incubation (Figure 2A).[305, 314] It should be noted that the microwave irradiation was applied intermittently to prevent overheating. Lin and Tseng showed that lysozyme from different vendors produced Au nanoclusters with different quantum yields, suggesting that salt and other small molecular contaminants may affect the synthesis.[306]

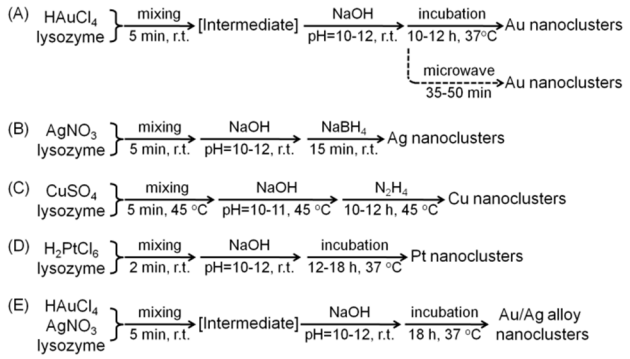

Figure 2. Synthetic protocols for metal nanoclusters with lysozyme in aqueous solutions. (A) Au nanoclusters,[155, 305] (B) Ag nanoclusters,[172] (C) Cu nanoclusters,[299] (D) Pt nanoclusters,[313] and (E) Au/Ag bimetallic alloy nanoclusters.[315] r.t.=room temperature.

Characterization and mechanism. The formation of Au nanoclusters can be indicated and easily monitored by the appearance of yellow-brown colour. Unlike monolayer protected Au nanoclusters, the lysozyme stabilized Au nanoclusters usually do not exhibit well-defined spectroscopic features (i.e., step-like fine structures) in UV-visible absorption spectra though an absorption band centred at 400 nm was observed.[306] The band of 400 nm was assigned to Au $5d^{10}$ to 6sp inter-band transitions and/or ligand-metal charge-transfer transitions.[306]

The formation of Au nanoclusters can be further confirmed and their sizes can be characterized by transmission electron microscopy (TEM), dynamic light scattering (DLS), and mass spectroscopy (MS).[155, 306, 309, 310, 312] Due to the ultrasmall sizes of the Au nanoclusters, high resolution TEM was usually employed.[155, 309, 310, 312] The size of the Au nanoclusters was around 1 nm under TEM (Figure 3).[155] As large as 4 nm nanoparticles were also observed, which was probably originated from the by-products (i.e., Au nanoparticles) rather than the Au nanoclusters.[312] The larger sizes measured by TEM might be also due to electron beam induced *in situ* aggregation of Au nanoclusters (or TEM sample preparation induced aggregation).

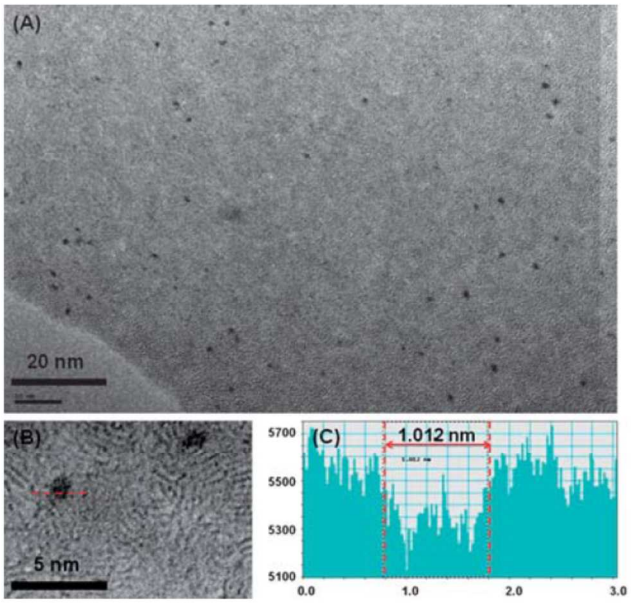

Figure 3. A typical TEM image of lysozyme stabilized Au nanoclusters (A), (B) the higher magnification image of panel (A), (C) the corresponding size of the particle line-crossed in panel (B). Reprinted with permission from ref.[155], copyright (2010) Royal Society of Chemistry.

The hydrodynamic sizes were measured by DLS.[306] Hydrodynamic sizes of 5, 7, 8, and 28 nm were reported, which was strongly dependent on the molar ratio of lysozyme to $HAuCl_4$.[306] Only the Au nanoclusters with the hydrodynamic size of 8 nm were discussed, which were prepared with a 0.17:1 molar ratio of lysozyme to $HAuCl_4$. Based on the dimension of lysozyme from crystal structure (i.e., 4.5 nm×3.0 nm×3.0 nm), it was suggested that a lysozyme monolayer was formed onto the Au nanocluster core.[306] However, this explanation was not consistent with the experimental results, which showed that the hydrodynamic sizes decreased from 28, 8, 7 to 5 nm when the molar ratios of lysozyme to $HAuCl_4$ increased from 0.14:1, 0.17:1, 0.21:1 to 0.28:1.[306] The explanation was also inconsistent with recent studies, which suggested that the Au nanocluster core was encapsulated within a lysozyme.[309, 310] If a monolayer of lysozyme proteins was formed onto the Au nanocluster core, the hydrodynamic size would increase with the increase of the molar ratios of lysozyme to $HAuCl_4$. Here, we proposed that each Au nanocluster was probably encapsulated within a lysozyme based on the previous studies.[306, 309, 310] This is in agreement with the measured hydrodynamic size of 5 nm for the Au nanoclusters from the 0.28:1 molar ratio of lysozyme to $HAuCl_4$. For the Au nanoclusters with large hydrodynamic sizes, the increased sizes might be originated from the aggregation of the Au nanoclusters encapsulated lysozyme due to salt or metal ions bridging.[309]

MS has been among one of the most suitable and powerful tools to elucidate the "actual molecular formulae" of ultrasmall nanoclusters.[219] Previous studies have demonstrated that various ionization modes can be used for nanoclusters MS analysis, such as electrospray ionization (ESI), laser desorption ionization (LDI), and matrix-assisted laser desorption ionization (MALDI), etc.[219] Among them, ESI-MS is the mildest mode with lowest fragmentation. However, the presence of metal nanoclusters makes the ESI-MS analysis of proteins very challenging. MALDI mode, combined with time-of-flight (TOF), thus was frequently employed in analyzing protein stabilized nanoclusters, including lysozyme stabilized metal nanoclusters.[121, 306, 309, 311, 316] Based on the MALDI data, Tseng and co-workers assigned a Au_{25} formula to the Au nanocluster stabilized by lysozyme, which emitted red fluorescence centered at ~657 nm (Figure 4).[121, 306] Note, as shown in the time-dependent fluorescent evolution profile in Figure 4, another emission peak centered at ~445 nm was observed, which was assigned as a Au_8 formula by Tseng et al.[121] Since multiple MALDI peaks with spacing of m/z 197 were detected for both the fluorescent species at 445 nm and 657 nm (referred as "blue fluorescent species" and "red fluorescent species", respectively), the two species were assigned to Au_8 and Au_{25} formulae based on Jellium model, respectively.[121] According to the model, the most stable metal clusters should have a magic number of atoms.[121] Later, Pradeep et al. performed a more detailed MALDI-MS analysis of the lysozyme stabilized Au nanoclusters.[309] For the "red fluorescent species", an m/z shift of 1970 from lysozyme alone was observed, suggesting the presence of 10 Au atoms within a single lysozyme (Figure 5). Therefore, it was claimed that a cluster of Au_{10} core was formed within a lysozyme protein. Careful analysis of the MALDI MS spectra in the entire mass range suggested that each Au nanocluster was confined within a lysozyme protein rather than grown between a few proteins.[309] For the "blue fluorescent species" made by incubating lysozyme and $HAuCl_4$ before exposure to basic conditions, Pradeep and co-workers detected a maximum of 3 Au atoms bound to a lysozyme using ESI MS.[309] The discrepancy of MS results between the above studies should be due to the typical fragmentation by using MALDI, which complicates the assignments.[219] Thus, more convincing data from other methods such as crystallography are needed to clarify the exact formulae of metal nanoclusters.

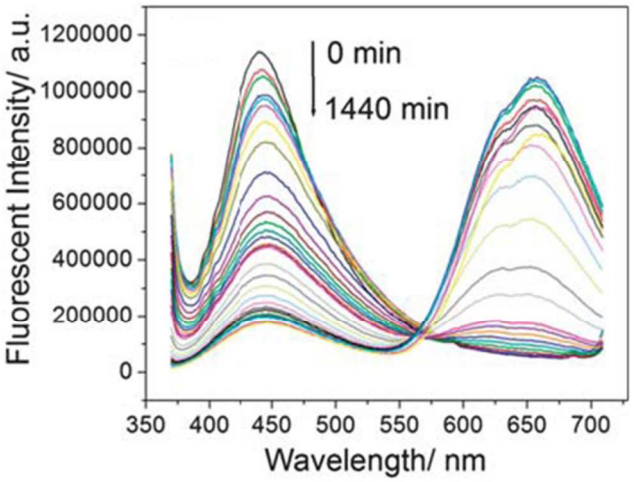

Figure 4. Time-dependent fluorescent spectra of lysozyme-stabilized Au fluorescent cluster. The excitation wavelength was 360 nm. Reprinted with permission from ref.[155], copyright (2010) Royal Society of Chemistry.

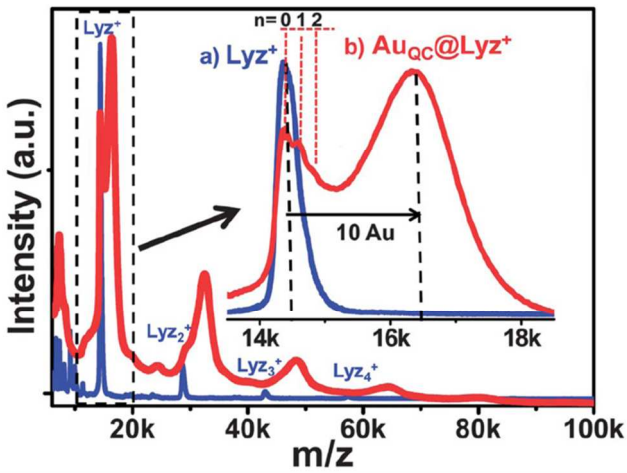

Figure 5. MALDI MS spectra of lysozyme (blue curves) and lysozyme-stabilized Au fluorescent nanocluster (red curves). Reprinted with permission from ref.[309], copyright (2013) Royal Society of Chemistry.

Nevertheless, as proposed by Wei et al. and echoed by Tseng's and Pradeep's groups, a growth mechanism can be proposed as follows: the mixing of lysozyme and $HAuCl_4$ at acid pH forms

intermediate species with blue fluorescence, it then converts to the final red fluorescence species when incubated at basic pH (Figures 2A and 6).[121, 155, 306, 309] More specifically, when lysozyme and $HAuCl_4$ are mixed at low pH, Au^{3+} binds to lysozyme through coordinating with amino acids' O and N atoms. The lysozyme-$(Au^{3+})_m$ complexes are then reduced to lysozyme-$(Au^{+})_m$ probably by carboxyl groups of acidic amino acids, as revealed by X-ray photoelectron spectroscopy (XPS) (*vide infra*), which would emit blue fluorescence. For lysozyme-$(Au^{+})_m$, Au^{+} may assemble together due to aurophilic attraction. At high pH, Au^{+} in lysozyme-$(Au^{+})_m$ is reduced to Au^0, which would further assemble into lysozyme-$(Au^0)_{m+n}$.[121, 155, 306, 309] Inter protein metal ions transfer was suggested since the regeneration of free lysozyme was detected during time-dependent MS analysis.[309] Circular dichroism (CD) spectra indicated that lysozyme at high pH had a more partially unfolded structure (i.e., less α-helical structure content) than lysozyme at low pH. The further unfolding of lysozyme would provide larger internal space for encapsulating enlarged Au nanocluster (Figure 6).[121] It was suggested that amine groups as well as thiols of cysteine were involved in stabilizing the formed Au nanocluster within lysozyme.[309, 310]

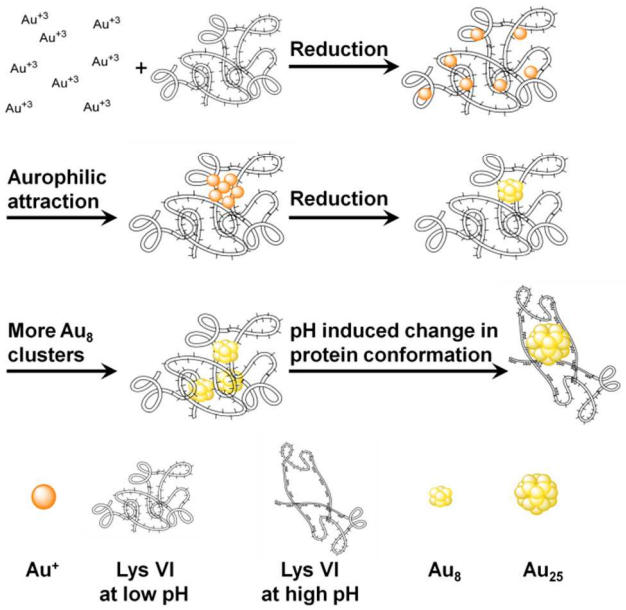

Figure 6. Proposed growth mechanism of lysozyme-stabilized Au fluorescent nanocluster. Adapted with permission from ref.[121], copyright (2012) John Wiley and Sons.

The photoluminescence quantum yields of the "red fluorescent species" were reported by several groups, ranging from 5.2% to 15.6%.[155, 306, 309, 310, 312] The variations might be due to the different measurement conditions as well as the quality of the nanoclusters synthesized. Lifetime measurements were also carried out in previous studies, showing the characteristic two lifetime components.[306, 309, 310]

As discussed above, XPS data showed that the "blue fluorescent species" should be lysozyme-$(Au^{+})_m$. For the "red fluorescent species", the collected XPS spectra could be deconvoluted into two distinct components, i.e., Au^{+} and Au^0.[155, 306] This indicated that the Au nanoclusters had a Au^0 core and Au^{+} shell. For Au_{25} with a Au_{13} core and 12 Au^{+}, the theoretical value of Au^{+} should be 48%. However, most of the measured values were lower, probably due to X-ray induced *in situ* reduction of Au^{+} during XPS measurements.

Besides CD spectroscopy (*vide supra*), infrared spectroscopy was also employed to investigate the potential structural changes of lysozyme after forming Au nanoclusters.[305, 309, 310, 312] Though the over spectrum of the lysozyme stabilized Au nanocluster was similar to that of lysozyme alone, a few changes were observed, indicating the increased unordered structures as well as fewer helical components.[305, 309, 310, 312]

It should be noted that the as-prepared Au nanoclusters were stable in as high as 500 mM NaCl and at high pH.[306]

Applications. Due to the unique fluorescent properties, the Au nanoclusters have been used to develop several sensing systems. As revealed by XPS, Au^{+} was present on the outside of the Au nanocluster. Due to the specific Au^{+}-Hg^{2+} interactions, the red fluorescence of the Au clusters was specifically quenched by Hg^{2+}. Based on this interesting phenomenon, selective and sensitive methods towards Hg^{2+} detection were successfully developed.[155, 306] It showed that CH_3Hg^{+} could also be determined with the Au nanoclusters.[306] It should be noted that the red fluorescence of the Au nanoclusters remained unchanged after exposure to glutathione (GSH), further suggesting the formation of a highly stable cluster (i.e., Au_{25}).[121]

Cyanide ions could etch the Au nanoclusters and thus quench the fluorescence. Based on this fact, Lu et al. employed the nanoclusters as new fluorescent probes to determine cyanide ions.[312]

Zhang's group found that the fluorescence of protein stabilized Au nanoclusters could be significantly enhanced on plasmonic substrates (such as nanostructured silver substrates).[307] The proteins used to direct formation of Au nanoclusters were BSA, human serum albumin (HSA), egg white albumin (EA), lysozyme and horseradish peroxidase (HRP). More interestingly, when these five nanoclusters immobilized onto a silver substrate were exposed to different target proteins, they produced distinct fluorescent patterns (Figure 7). Using this sensing array strategy, as many as 10 proteins with 0.2 μM were successfully identified.[307]

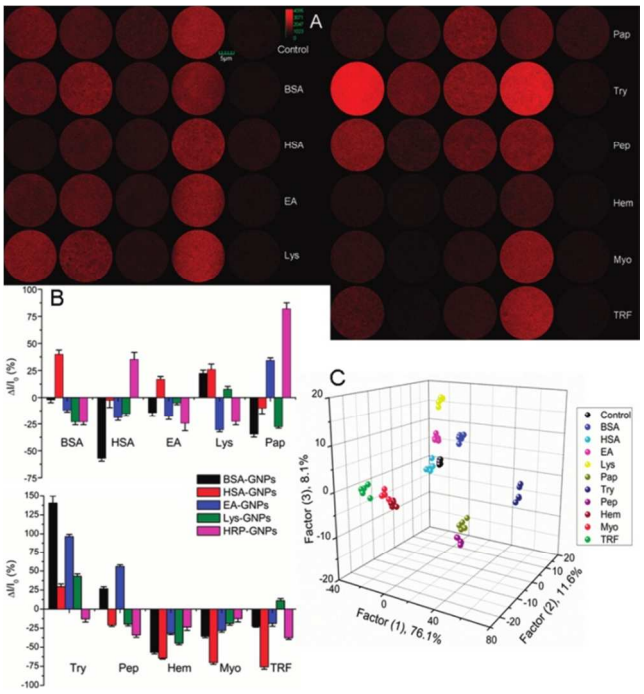

Figure 7. Combined with others protein stabilized clusters, lysozyme stabilized Au nanoclusters were fabricated into a sensing array on a plasmonic substrate for protein detection. Reprinted with permission from ref.[307], copyright (2012) American Chemical Society.

Since the bioactivity of lysozyme was retained after forming the Au nanoclusters, the lysozyme stabilized Au nanoclusters were able to recognize and to label bacteria, as demonstrated by Chen et al.[305] As shown in Figure 8, the Au nanoclusters were able to bind onto and thus label pan-drug-resistant *Acinetobacter baumannii* (PDRAB) and vancomycin-resistant *Enterococcus faecalis* (VRE), two typical antibiotic-resistant bacteria. The Au nanoclusters also interacted with Gram-negative bacteria and Gram-positive bacteria, such as *E. coli* and *S. aureus*, showing their potential use as broad-spectrum labeling probes for pathogenic bacteria.[305] Though thiols of cysteines and amine groups may be involved in stabilizing the Au nanoclusters, no cysteine is located within the active sites of lysozyme at Glu-35 and Asp-52.[305] Thus, the lysozyme's bioactivity of the Au nanoclusters was retained as demonstrated above. When the antimicrobial activity against VRE and PDRAB was examined, it was found that the Au nanoclusters showed better performance (i.e., more effective inhibition of bacteria cell growth) than free lysozyme.[305] This may be originated from the synergic effects.

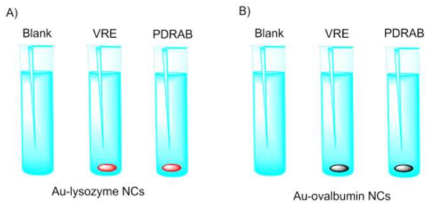

Figure 8. Lysozyme stabilized Au nanoclusters for bacterial labeling. The images were taken under illumination of a ~365 nm UV lamp. NC: nanocluster; PDRAB: pan-drug-resistant *Acinetobacter baumannii*; VRE: vancomycin-resistant *Enterococcus faecalis*. Adapted from ref.[305].

Chen et al. later showed that lysozyme stabilized Au nanoclusters could be also used to concentrate target bacteria. The concentrated bacteria were then analyzed and identified by MALDI MS assisted with principal component analysis (PCA). As low as ~10^6 cells/mL was successfully detected by the proposed method.[314]

Nanozymes are nanomaterials with enzyme-like activity.[33] Recently, it showed that lysozyme stabilized Au nanoclusters possessed peroxidase-like activity. When the Au nanoclusters were conjugated onto folic acids functionalized graphene, the conjugates could be used for cancer cell detection. With this sensing platform, as few as 1000 MCF cells were detected.[308]

2.1.2 Ag

Synthetic protocols. Compared with Au nanoclusters, the synthesis of silver nanoclusters is more challenging due to their intrinsic chemical instability.[117] As promising fluorescent probes, considerable efforts have been devoted to silver nanoclusters preparation recently.[117, 210] Several protein-stabilized silver nanoclusters have been synthesized.[115, 117, 317] As shown in Figure 2B, a facile approach to red-emitting silver nanoclusters was developed.[172] The synthesis was carried out by reducing silver nitrate with $NaBH_4$ in the presence of lysozyme under basic conditions, which would partially unfold the lysozyme protein and provide more space for encapsulating the nanocluster formed. The alkaline reaction solution would also help to cleave disulfide bonds and liberate free cysteines. The freed cysteines could act as polyvalent ligand to stabilize the silver nanoclusters. As noted, the freshly prepared silver nanoclusters were not stable at high pH. So they were transferred to neutral pH solution for long-term storage.[172]

Characterization and applications. The synthesized silver nanoclusters had a size of 1.5 nm under TEM and a hydrodynamic size of 7 nm. No MS spectra have been obtained for the nanoclusters. Due to the high pI of lysozyme (pI=11.3), the nanoclusters had a zeta potential of about +30 mV at neutral pH. Interestingly, the silver nanoclusters emitted red fluorescence at 605 nm. A quantum yield of 1.3% was reported.[172] XPS measurements revealed the co-existence of Ag^0 and Ag^+. Due to the specific Ag^+-Hg^{2+} metallophilic interaction, the silver nanoclusters were used as sensitive and selective probes for Hg^{2+} sensing.[172]

2.1.3 Others

Several other metal nanoclusters stabilized by lysozyme were also reported, including copper, platinum, and alloy.[299, 313, 315]

Copper nanoclusters. Blue-emitting copper nanoclusters were synthesized by reducing copper sulfate with hydrazine in the presence of lysozyme under basic conditions (Figure 2C).[299] The TEM images indicated that the ~0.96 nm small nanoclusters were aggregated into ~2.3 nm assemblies. CD and IR spectra again showed the disturbed lysozyme structures after forming the copper nanoclusters.[299, 305, 309, 310, 312] The fluorescent quantum yield of the emission at 450 nm was measured to be 18% when the nanoclusters were excited at 360 nm. Interestingly, the nanoclusters' fluorescent emission wavelength was dependent on

the excitation wavelength (Figure 9A), implying that multiple species were present.[299] MALDI MS analysis indeed showed the presence of multiple species, such as Cu_2, Cu_4 and Cu_9 (Figure 9B).[299] The copper nanoclusters did not show significant cytotoxicity. When co-incubated with cancer cells, such as Hela cells, the copper nanoclusters were uptaken by the cells and could be used for cell labelling and imaging.[299] The preliminary data showed that the copper nanoclusters were stable in blood and did not cause obvious hemolysis.[299]

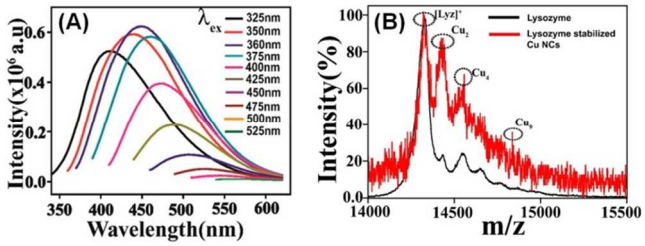

Figure 9. (A) Fluorescent spectra and (B) MALDI-TOF MS of the lysozyme stabilized copper nanoclusters. Reprinted with permission from ref.[299], copyright (2014) American Chemical Society.

Platinum nanoclusters. The above synthetic protocol was recently extended to platinum nanoclusters.[313] As shown in Figure 2D, the lysozyme stabilized ultrasmall platinum nanoclusters with blue fluorescence could be created by incubating lysozyme and H_2PtCl_6 under basic conditions. The platinum nanoclusters were too small to be imaged with TEM. When MALDI TOF MS analysis was conducted, a Pt_4 formula was revealed, confirming the ultrasmall size of the nanoclusters. When excited at 370 nm, the nanoclusters emitted blue fluorescence at 434 nm with a quantum yield of 0.08 and a fluorescence lifetime of 3.0 ns. The fluorescence was excitation wavelength dependent. Similar to the Au nanoclusters mentioned above, the platinum nanoclusters were also composed of 67% Pt^+ and 33% Pt^0, as identified by XPS measurements. The presence of Pt^0 was further testified by the fact that the platinum nanoclusters' fluorescence could be quenched by Hg^{2+}.[313]

Interestingly, the platinum nanoclusters exhibited an intrinsic oxidase-like activity. It showed that the platinum nanoclusters could catalyze the oxidation of 2,2'-azino-bis(3-ethylbenzothiazoline-6-sulphonic acid) (ATBS), 3,3',5,5'-tetramethylbenzidine (TMB), and dopamine in the presence of O_2. The platinum nanoclusters had higher oxidase mimic activity when compared with platinum particles larger than 5 nm.[313] The degradation of methylene blue in lake water was explored by using the platinum nanoclusters as oxidase mimic. Methylene blue was indeed degraded in the presence of the platinum nanoclusters, showing the great promise in future water treatment.[313]

Alloy nanoclusters. As discussed above, Tseng et al. suggested the formation of intermediate Au_8 nanoclusters in the conversion of lysozyme-$(Au^+)_m$ to lysozyme-$(Au^0)_{m+n}$ (i.e., Au_{25}, as proposed by them) (Figure 2A).[121] Later, they found that the presence of Ag^+ ions in the reaction solution slowed down the conversion, and thus produced both small and large sized metal nanoclusters simultaneously (Figure 2E).[315] The formation of alloyed nanoclusters was indicated by the blue shift of the first exciton absorption and fluorescence peaks and confirmed by the MALDI MS analysis. By analyzing the MS spectra, the small nanoclusters were assigned as Au_7Ag and Au_8 while the large ones as $Au_{24}Ag$. Since the small nanoclusters were insensitive to Hg^{2+} while the large ones were sensitive to Hg^{2+}, a ratiometric fluorescence assay towards Hg^{2+} was proposed (Figure 10). Such ratiometric sensing protocol would overcome the potential interfering factors such as environmental variations and photo bleaching, etc. The Hg^{2+} concentration in tap water was evaluated by the proposed assay.[315]

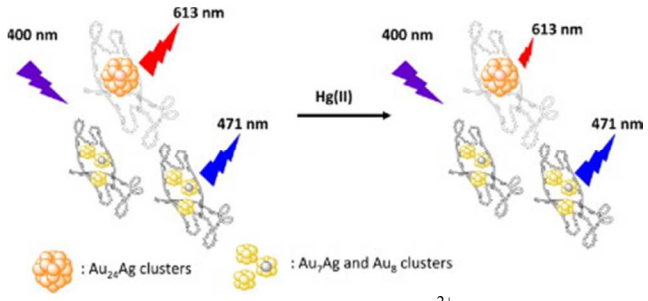

Figure 10. Ratiometric sensing of Hg^{2+} using two-sized nanoclusters. Reprinted with permission from ref.[315], copyright (2013) Elsevier.

2.2 Metal nanoparticles

Protein-directed approach has also been extensively explored to synthesize varieties of functional metal nanomaterials.[175, 182] Nanostructured gold, silver, copper, nickel, cobalt, platinum, and palladium, etc. have been prepared with different proteins, such as BSA, bacteriophage T4 gene product 5 trimers with histidine tags, cytochrome c, ferritin, heat shock protein, hemoglobin, HSA, mosaic virus proteins, etc.[175, 318-323] The as-prepared nanomaterials are biocompatible and have been widely used such as in biosensing, bioimaging, cancer therapy, catalysis, etc. Lysozyme has also been employed to direct synthesis of metal nanoparticles, including gold and silver nanoparticles in solution phase.[171, 322, 324-327]

2.2.1 Au

Synthetic protocols. As shown in Figure 11, lysozyme protected Au nanoparticles can be synthesized via wet chemistry approaches. For example, Li's group developed a facile way to synthesis of lysozyme monolayer protected Au nanoparticles by reducing $HAuCl_4$ with $NaBH_4$ in the presence of lysozyme (Figures 11A and 13A).[171] The as-prepared Au nanoparticles have a size of 2.4 nm. Hydrodynamic size measurement indicated that a monolayer of lysozyme was assembled onto the Au core.[171] Around 15-20 nm Au nanoparticles could be obtained by simply heating the mixture of $HAuCl_4$ and lysozyme (Figure 11B).[322, 326] Since no extra reducing agents were introduced, the protein itself should act as the reducing agents. When a kitchen microwave oven was employed for synthesis (Figure 11C), the reaction time was shorten to 2 min. Larger Au nanoparticles with a size of 34.5 nm were obtained.[325] The microwave overheating may actually denature the lysozyme used and liberate free cysteines for stabilizing the Au nanoparticles.[325]

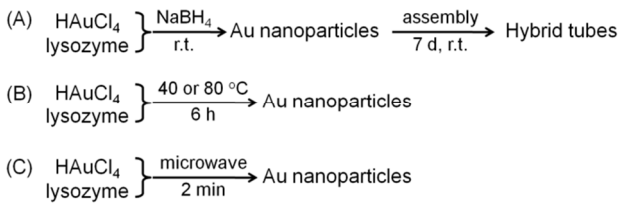

Figure 11. Synthetic protocols for Au nanoparticles with lysozyme in aqueous solutions.

Mechanism. Understanding the interactions between lysozyme and Au nanoparticle core and potential conformational changes of lysozyme induced by the nanoparticles formation are critical to elucidate the mechanism. Surface enhance Raman scattering (SERS) was used by Das et al. to investigate the mechanism of lysozyme capped Au nanoparticles (synthesized as shown in Figure 11B at 40 °C).[326] Since the lysozyme was in the proximity of the Au nanoparticles core, enhanced Raman signals from lysozyme could be probed. The characteristic peaks at 1484, 1545, and 1583 cm^{-1}, corresponding to phenylalanine, tyrosine, tryptophan, and histidine residues, were observed, suggesting the stabilizing roles of these residues (Figure 12). The presence of the peak at 1289 cm^{-1}, assigned to amide III band, confirmed the assembly of lysozyme monolayer onto the Au nanoparticles.[326] Note, IR spectra also showed the presence of amide I, amide II, and amide III bonds. Interestingly, though the protein was partially denatured, the S-S bonds peak at 509 cm^{-1} was observed, indicating the disulfide bonds remained intact.[326]

Self-assembly. Li and co-workers later serendipitously found that the lysozyme stabilized Au nanoparticles self-assembled into microtubes when they were aged for one week at ambient conditions (Figure 13B).[171, 324] The tubes had a diameter of 1-2 μm with Au nanoparticles decorated onto them. It was suggested that hydrogen bonding originated from amino acid residues of lysozyme may mediate the assembly.[324]

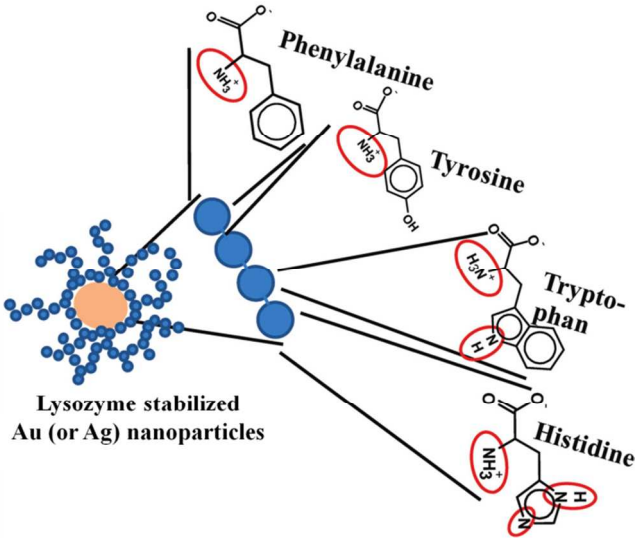

Figure 12. SERS was adopted to elucidate the mechanism of lysozyme capped Au and Ag nanoparticles, showing certain amino acids played critical roles in stabilizing the nanoparticles. Reprinted with permission from ref.[326], copyright (2009) American Chemical Society.

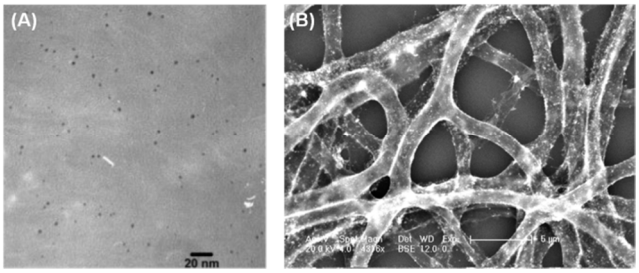

Figure 13. Lysozyme monolayer-stabilized Au nanoparticles (A) and their self-assemblies into hybrid tubes (B). Reprinted with permission from ref.[171], copyright (2007) American Chemical Society (A); and ref.[324], copyright (2011) American Chemical Society (B).

Cellular study. As high as 200 μg/mL of Au nanoparticles capped by lysozyme showed no detectable cytotoxicity, which was evaluated by MTT assay, demonstrating the excellent biocompatibility.[325] Uptaken by mouse embryonic fibroblast NIH-3T3 cells, the nanoparticles were accumulated in both cytoplasm and nucleus. The inhibition studies revealed that the Au nanoparticles were uptaken via receptor-mediated endocytosis, specifically, the clathrin-dependent endocytosis.[325]

2.2.2 Ag

Synthetic protocols. As discussed above (Figure 12), lysozyme stabilized Ag nanoparticles were also synthesized via the wet chemistry approach.[325] The SERS analysis revealed that several key amino acid residues, such as phenylalanine, tyrosine, tryptophan, and histidine residues, were involved in interacting with the Ag nanoparticle core. Notably, the Ag-N bonding peak at 236 cm^{-1} was observed, suggesting the potential coordination with Ag nanoparticles via nitrogen atoms in the amino acid residues.[325]

An interesting lysozyme catalytic method to prepare Ag nanoparticles was reported.[328] When the mixture of lysozyme and silver acetate in methanol was exposed to light, the Ag nanoparticles were formed after about 1 hour exposure. Note, no colloid stable Ag nanoparticles formed in aqueous solution instead. By controlling the molar ratios of silver acetate to lysozyme, more monodispersed Ag nanoparticles of 8 nm were obtained. The as-prepared Ag nanoparticles in methanol were successfully transferred into aqueous solution by solvent exchange with dialysis. The Ag nanoparticles in aqueous solution had as long as 6 months storage stability.[328] IR spectra indicated the presence of lysozyme in the Ag nanoparticles aqueous solution even after dialysis, and DLS measurement confirmed the presence of a lysozyme monolayer onto the Ag nanoparticle core.[328]

Antimicrobial activity. The hydrolysis of a synthetic substrate mimic indicated that the lysozyme after Ag nanoparticles formation retained its activity as a hydrolase.[328] Then, the antimicrobial activity of the lysozyme stabilized Ag nanoparticles was evaluated. Remarkably, they inhibited the growth of several bacterial and fungal strains, such as *E. coli*, *S. aureus*, *B. anthracis*, and *C. albicans*. More strikingly, they even exhibited significant antimicrobial activity against *P. mirabilis strains* (LST149 and LST 169A) and *a recombinant E. coli strain* (J53/pMG101), which were usually antibiotic- and silver-

resistant.[328] The toxicity towards mammalian cells was also tested, showing the Ag nanoparticles were nontoxic at the antimicrobial concentrations. The Ag nanoparticles may find wide applications in aseptics and therapeutics in the future.

2.3 Others nanomaterials

Many other nanomaterials, including calcium carbonate, metal oxides, metal sulfides, metal tellurides, and composites, have been synthesized by using lysozyme.[160, 161, 163, 165, 170, 329-340]

2.3.1 $CaCO_3$

Calcium carbonate ($CaCO_3$), one of the major biogenic minerals, is widely found in biomineralizing organisms' exoskeletons and tissues, providing them unique mechanical strength and well-defined shapes and structures.[330, 331] Avian eggshells are excellent examples of biogenic minerals with hierarchically assembled porous structures, consisting of $CaCO_3$ and biomacromolecules. In an eggshell, $CaCO_3$ exists in the anhydrous form of crystalline calcite, the most thermodynamic stable form.[330] Though extensive efforts have been devoted to understanding the formation mechanism of eggshell, it still remains elusive due to the complexity. Many studies suggested that lysozyme, one of the key egg white proteins (~3.5%), plays a pivotal role in the calcification of eggshell.[329-333] Lysozyme mediated $CaCO_3$ *in vitro* biomineralization has been investigated by several groups.

Kinetics and time-dependent morphologies were examined to understand the effects of lysozyme on the precipitation of $CaCO_3$. It showed that lysozyme could promote the nucleation of $CaCO_3$ while the waiting time for precipitation was prolonged in the presence of lysozyme. Interestingly, the presence of lysozyme affected the habit (i.e., the external shape) of the calcite crystals formed. Without lysozyme, the calcite crystals exhibited rhombohedra morphology. At the lower concentrations of lysozyme, the rhombohedra morphology was still dominant. At the mediate and higher concentrations of lysozyme, the rhombohedra morphology was converted into calcite with {110}, {100}, and {104} facets, and finally into spherical calcite aggregates, due to the sequentially inhibiting growth of {110}, {100}, and {001} facets.[333]

Usually, the final crystalline calcite is transformed from an intermediate form of $CaCO_3$ by dissolving and recrystallizing the intermediate. Previous studies indicated that lysozyme adsorbed may attract and concentrate calcium ions and thus provide local nucleation sites. Such interactions between lysozyme and $CaCO_3$ favoured the nucleation and led to smaller but more interconnected amorphous $CaCO_3$, compared with lysozyme-free system.[330, 331, 333] Lu et al. have investigated the lysozyme mediated $CaCO_3$ biomineralization by diffusion growth of $(NH_4)_2CO_3$ vapour into $CaCl_2$ aqueous solution. Scanning electron microscopy (SEM) and X-ray diffraction (XRD) measurements clearly revealed the transformation from hexagonal and spherical vaterite (the most unstable form of $CaCO_3$) into coexistent calcite and vaterite, and finally into pure calcite, demonstrating the directing role of lysozyme in the formation of biomineralized $CaCO_3$ (Figure 14).[330]

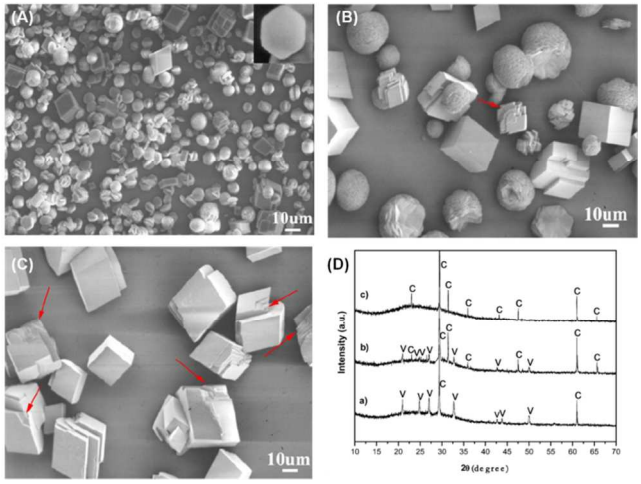

Figure 14. Lysozyme mediated calcium carbonate biomineralization. SEM images of $CaCO_3$ formed after 12 h in the absence (A) and presence of 0.5 g/L lysozyme (B) and 2 g/L lysozyme (C), respectively. (D) The corresponding X-ray powder diffraction patterns of the formed $CaCO_3$. Reprinted with permission from ref.[330], copyright (2009) Elsevier.

2.3.2 Oxides

Silica. Silica (SiO_2) nanoparticles can be prepared by hydrolysis of the precursors, such as tetramethyloxysilane (TMOS), tetraethyloxysilane (TEOS) and their analogues.[341-343] The hydrolysis can be catalyzed and tuned by acids, bases, and other catalysts. Researchers have established that lysozyme could assist the hydrolysis reactions for forming silica particles.[161, 165, 334, 344-347] Johnson et al. showed that lysozyme could template and significantly accelerate the precipitation of silica via a catalytic biomineralization approach (Figure 15A).[334, 344] Minimal concentration of lysozyme was needed for visible silica formation. More, the formation rate and yield of the silica particles could be tuned by changing the amount of lysozyme used. The higher concentration of lysozyme was used, the higher rate and yield were obtained.[334, 344] They also found that the lysozyme still retained its antimicrobial activity (such as lysis of the cell wall of *M. lysodeikticus*) even it was physically embedded within the silica matrix. The thermal stability was enhanced when compared with free lysozyme.[334] Interestingly, SEM and TEM images suggested the silica particles had a hierarchical architecture, i.e., spherical particles of 8-10 nm self-assembled into large particles of 460 nm (Figures 15A and 15B). The large particles were dominant in spherical shape, although other shapes, such as ellipsoid and polyhedral structures, were also observed. To further elucidate the exact interactions of lysozyme and silica matrix, small angle neutron scattering (SANS) with contrast matching technique was employed. As shown in Figure 15B, the SANS data revealed that the primary building blocks of the final hierarchical architecture were the assembled clusters (3.3 and 8.5 nm) from lysozyme (1.8 nm) and silica nanoparticles (1.3 nm). The primary building blocks then aggregated together to form the as large as 460 nm final silica particles.[334]

Interestingly, reaction conditions (such as stirring versus sonication) played key roles in controlling the morphology of the silica in the presence of lysozyme.[165, 346, 347] The hydrolysis

reaction under stirring produced granular silica particles. However, when sonication was applied, hollow spherical particles of 0.5-15μm with the shell thickness of 100 nm were formed.[165, 346, 347] As proposed by Sakaguchi et al., the hollow structures were formed via the following mechanism: first, sonication would induce the formation of TEOS emulsion droplets, which was covered with lysozyme. Then the lysozyme would *in situ* catalyze the hydrolysis and form lysozyme-silica shell structures. The leaked TEOS from the droplets would be further catalytically hydrolyzed by lysozyme, which resulted in the increase of particle shell thickness. When the lysozyme used was not sufficient, the sonication would decrease the droplet size and thus the final silica size. On the other hand, when excess lysozyme molecules were present, the single particles would grow together and form aggregates or sponge-like structures.[165] The further post-treatment of the hollow silica structures by calcination would produce either mesoporous silica (500 °C) or cage-like hollow silica spheres (700 °C).[346]

Titania. The lysozyme catalyzed hydrolysis of the corresponding precursors, such as potassium hexafluorotitanate (PHF-Ti) and titanium(IV) bis(ammonium lactato)dihydroxide (Ti-BALDH), provides a rapid and facile method to fabricate titania (TiO_2) particles under ambient conditions.[161] The lysozyme molecules were entrapped simultaneously within the titania matrix during the hydrolysis reaction. The entrapped lysozymes retained their antimicrobial activities. Additional enzymes could also be co-entrapped. For example, butyrylcholinesterase was encapsulated within the titania/lysozyme hybrids during the titania precipitation and retained its enzymatic activity. More, the encapsulated enzymes showed enhanced thermal stability compared with the free ones. For both titania particles from PHF-Ti and Ti-BALDH, selected area electron diffraction (SAED) and XRD measurements confirmed that they were amorphous. Interestingly, different precursors would produce titania with different sizes, compositions and morphologies. For example, titania from PHF-Ti gave polydispersed particles with size of 100 nm to 1 μm, while titania from Ti-BALDH produced fine particles of 10-50 nm. Also, the later had higher lysozyme content than the one from PHF-Ti. The slightly lower activity of entrapped lysozymes compared with free ones was attributed to the physical steric hindrance after entrapment.[161]

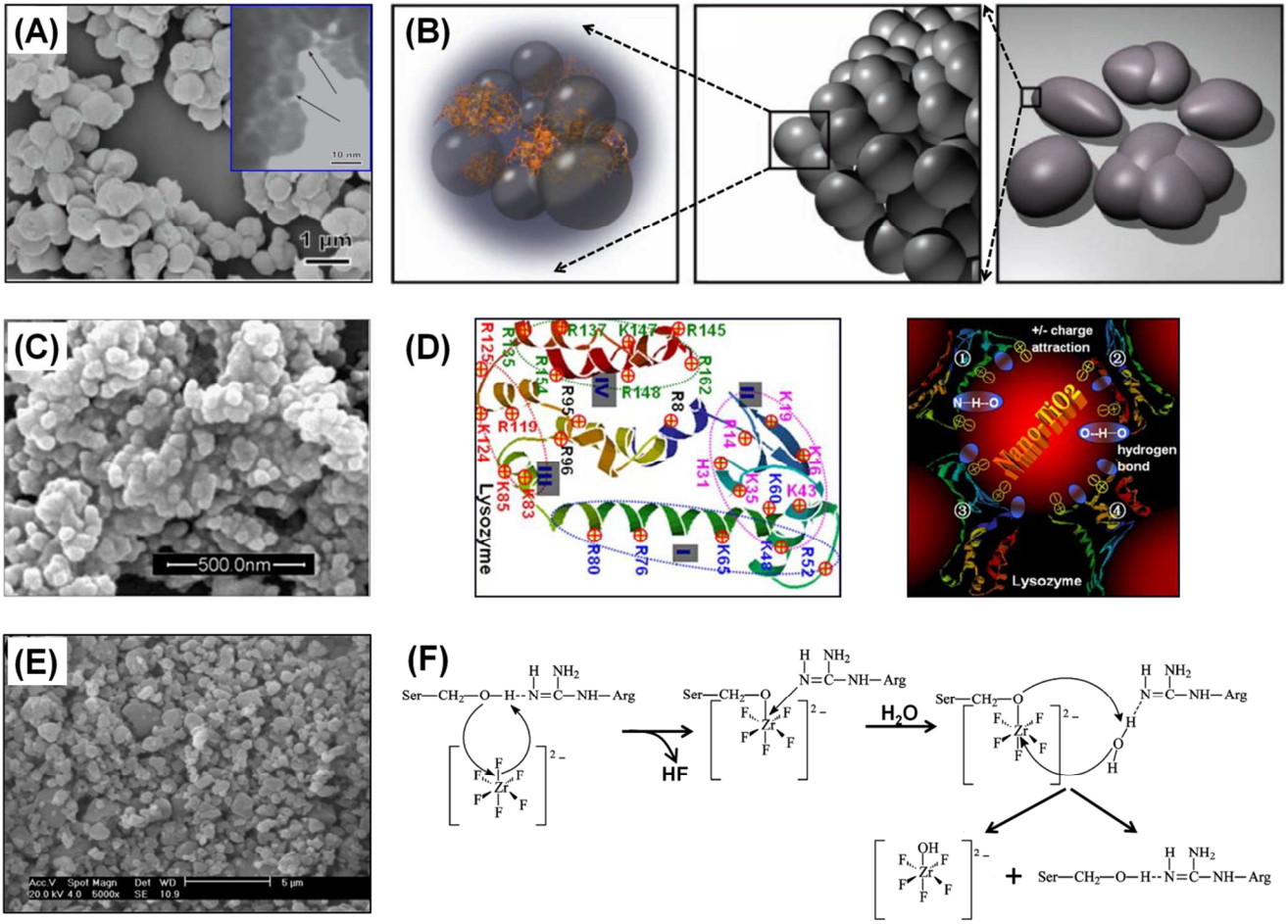

Figure 15. Lysozyme directed approaches to oxides. (A) SEM and TEM (inset) images of silica formed by hydrolysis of TMOS; (B) schematic of hierarchical assembly of the silica particles; (C) SEM image of titania-lysozyme nanoparticles; (D) the proposed interactions of lysozyme and the titania nanoparticles; (E) SEM image of zirconia formed by hydrolysis of K_2ZrF_6; (F) the proposed mechanism of lysozyme-directed forming zirconia. Reprinted with permission from ref.[334], copyright (2010) John Wiley and Sons (A and B); ref.[160], copyright (2009) Springer (C and D); and ref.[335], copyright (2008) American Chemical Society (E and F).

When studying the interactions of lysozyme and prepared titania nanoparticles of 60 nm, Gao et al. found that the titania

nanoparticles affected the enzymatic activities of lysozyme (Figure 15C). Based on the detailed studies, a two-step binding mode was proposed to interpret the phenomenon. The negatively-charged titania nanoparticles interacted with positively-charged lysozymes electrostatically first. After the initial binding, the proximity of lysozymes to the surface of titania nanoparticles would induce the formation of new hydrogen bonds (such as N-H···O and O-H···O) (Figure 15D). Such bridges between the titania nanoparticles and lysozyme monolayers would induce local deformation of the absorbed lysozymes and thus decrease the enzymatic activity as observed.[160]

Zirconia. Zirconia (ZrO_2) particles were prepared by catalytic hydrolysis of K_2ZrF_6 in the presence of lysozyme at room temperature.[335] Irregular particles with a size of 1 μm rather than small nanoparticles were obtained, probably due to the rapid hydrolysis catalyzed by lysozyme (Figure 15E). Careful characterization with energy-dispersive X-ray spectrometry (EDX), thermogravimetric analysis (TGA), IR and XPS, confirmed the formation of zirconia particles. Interestingly, thermally denatured lysozyme could also catalyze the hydrolysis, indicating some amino acid residues of the side chains (rather than the residues of the active site) were responsible for the lytic reaction (Figure 15F). More, when other enzymes, such as yeast alcohol dehydrogenase (YADH), were introduced in the reaction precursor solution of lysozyme and K_2ZrF_6, the enzymes could be incorporated in the zirconia particles. The incorporated enzymes showed enhanced thermal and pH stability.[335]

2.3.3 Metal sulfides and tellurides

Several metal sulfides stabilized by lysozyme have been synthesized by Qin et al.[336-338] Cubic zinc blende phase of ZnS nanoparticles with spherical shape were prepared by using zinc acetate and thioacetamide as precursors in the presence of lysozyme aqueous solution. The ZnS particles had an average size of around 40 nm. IR spectra suggested that the -OH and -NH groups of lysozyme may be involved in interacting with the ZnS nanoparticles.[336] Using a very similar approach, cubic PbS nanoparticles with an average size of 45 nm were also synthesized. Interestingly, the photoluminescence spectrum centred at 470 nm was obtained, which was probably originated from sulphur vacancy defects.[337] Photoluminescence tuneable HgS nanoparticles could also be obtained by changing the ratio of lysozyme to the precursors used. The smaller HgS nanoparticles with stronger photoluminescence were gotten for higher lysozyme concentrations (i.e., HgS nanoparticles with the average size of 14, 19, and 27 nm were obtained with 5, 3, and 1 mg/mL lysozyme, respectively).[338] Gao and co-workers showed that single-crystalline bismuth sulfide and bismuth oxide nanowires with length of micrometers could be fabricated under mild conditions with a lysozyme-assisted approach. Bismuth sulfide nanowires had diameters of 10-50 nm while bismuth oxide had an average diameter of 8 nm. The coordination between Bi^{3+} and certain groups of lysozyme may play a key role in directing the formation of nanowires rather than other irregular shapes.[348]

Using the evaporation-induced self-assembly method, microscaled dendrite structures were fabricated from the mixture of thioglycolic acid capped CdTe quantum dots (~2.3 nm) and different proteins (including lysozyme) on glass substrates. The dendrite structures could be fine-tuned by controlling the pH of reaction solution and by introducing metal ions.[163]

2.3.4 Composites

Nanocomposites are nanomaterials with multiple components, which are usually effectively integrated. Compared with mono-component nanomaterials, nanocomposites may have enhanced properties due to the synergistic effects. Liu et al. showed that ternary TiO_2-SiO_2-Ag nanocomposites indeed exhibited enhanced visible-light photocatalytic activity towards Rhodamine B degradation.[170] The nanocomposites were made step-wisely via a facile lysozyme-directed approach (Figure 16). Specifically, TiO_2 nanoparticles of ~280 nm were first formed by lysozyme induced hydrolysis of Ti-BALDH. It was suggested that the positively charged arginine and lysine residues of lysozyme interacted with Ti-BALDH electrostatically and thus induced the hydrolysis. Then, the TiO_2-SiO_2 composites were obtained by forming SiO_2 patch layers from sodium silicate onto the surface of the as-prepared TiO_2 nanoparticles. Finally, Ag nanoparticles of ~25 nm were *in situ* produced and deposited on the TiO_2-SiO_2 composites by reduction of Ag^+ with the reducing residues of lysozyme (such as tryptophan, tyrosine, phenylalanine, and histidine residues). The formation of the TiO_2-SiO_2-Ag nanocomposites was confirmed by EDX elemental mapping and TEM imaging as well as other characterizations. Due to the synergistic effects of enhanced light harvesting from plasmonic Ag nanoparticles and increased adsorption capacity of dyes (Rhodamine B here) from SiO_2, the highest degradation rate of 0.841 h^{-1} was observed for the TiO_2-SiO_2-Ag nanocomposites. As a comparison, the rates for TiO_2, TiO_2-SiO_2, and TiO_2-Ag nanomaterials were 0.098 h^{-1}, 0.448 h^{-1}, and 0.330 h^{-1}, respectively. The ternary nanocomposites could be recycled due to the strong chemical stability.[170]

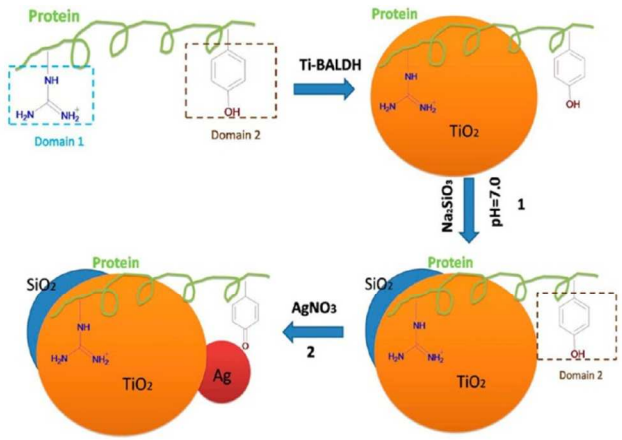

Figure 16. Lysozyme was used to direct the synthesis of TiO_2-SiO_2-Ag nanocomposites. Reprinted with permission from ref.[170], copyright (2013) American Chemical Society.

3. Lysozyme crystals

Though protein crystals, especially protein single crystals, are traditionally grown to obtain structural information in molecular biology, researchers have established that they can be regarded as novel porous materials.[10, 108, 110, 114, 157, 159, 162, 164, 169, 189, 190, 349-355] When treated as emerging materials, protein crystals have several unique features compared with other materials and their

assemblies.[10, 108, 114, 157, 159, 162, 164, 169, 189, 190, 349-354, 356-360] First, they have highly ordered 3D structures periodically assembled from the corresponding protein monomers. Second, they are porous materials with precisely controlled pore sizes. The pores are usually filled with solvents such as aqueous buffer solutions. These solvent channels can be used as templates to grow nanomaterials and to encapsulate guest molecules. Third, the amino acid residues exposed to the solvent channels can interact with incoming species (such as coordinating with metal ions added), which in turn may direct and tune the formation of designed materials. Fourth, the formed materials (or encapsulated guest molecules) in the porous channels and the host protein crystals have synergic effects, rendering the hybrid materials with enhanced or even new properties. Fifth, the single crystals of proteins may provide atomic resolution structural information and thus help understanding the mechanisms involved. Although protein crystals are inherently fragile and the growth of protein crystals is usually very challenging, controllable manipulation of protein crystals are now achievable thanks to substantial progress in the field of protein crystal engineering.[108, 189, 190] Recently, rapid progresses have been made in directing synthesis of functional nanomaterials with protein crystals.

In this section, the use of lysozyme crystals (in both cross-linked and intact native forms) to direct synthesis of different kinds of hybrid nanomaterials is discussed.

3.1 Metal nanomaterials

3.1.1 Au

Mann et al. reported the synthesis of plasmonic metal nanomaterials within cross-linked lysozyme crystals.[114] The cross-linked lysozyme crystals were obtained by soaking the native lysozyme single crystals in the crystallization buffer solution containing glutaraldehyde. Arrays of plasmonic Au nanofilaments were then obtained by sequestrating $HAuCl_4$ into the cross-linked lysozyme crystals, followed by *in situ* reduction with $NaBH_4$. The formation of plasmonic Au nanostructures could be easily followed by the colour change of the crystals (Figure 17). Diffuse reflectance UV-visible spectroscopic measurements revealed two absorbance peaks centred at around 583 and 684 nm, clearly confirming the formation of plasmonic Au nanostructures. The two peaks were assigned to the transverse and longitudinal plasmon resonance bands, respectively. TEM images further confirmed the formation of Au nanofilaments infiltrated within the porous channels of the cross-linked lysozyme crystals. IR spectra indicated that the presence of Au nanostructures did not affect the protein structures significantly. Though the crystals' tetragonal morphology remained effectively unchanged after the formation of Au nanostructures, some crystals were cracked (Figure 17). Single crystal X-ray diffraction measurements showed that the hybrid crystals only exhibited low intensity reflections, which was probably associated with a disordered tetragonal phase.[114]

Later, they performed a more detailed study to investigate the optical response of the infiltrated Au nanostructures within the cross-linked lysozyme crystals. Using angle- and polarization-dependent spectroscopy, they showed that the encapsulated Au nanostructures were isolated with spheroidal or slightly anisotropic shapes.[354] No continuous nanowires were detected inside the crystal host. The plasmonic response was attributed to the isolated Au nanostructures. Interestingly, the fluorescent measurements suggested the presence of ultrasmall Au clusters, which emitted light around 650-750 nm.[354] The simultaneously formation of both plasmonic and fluorescent Au nanostructures with the cross-linked lysozyme crystals may provide a new approach to synthesis of multi-functional materials.

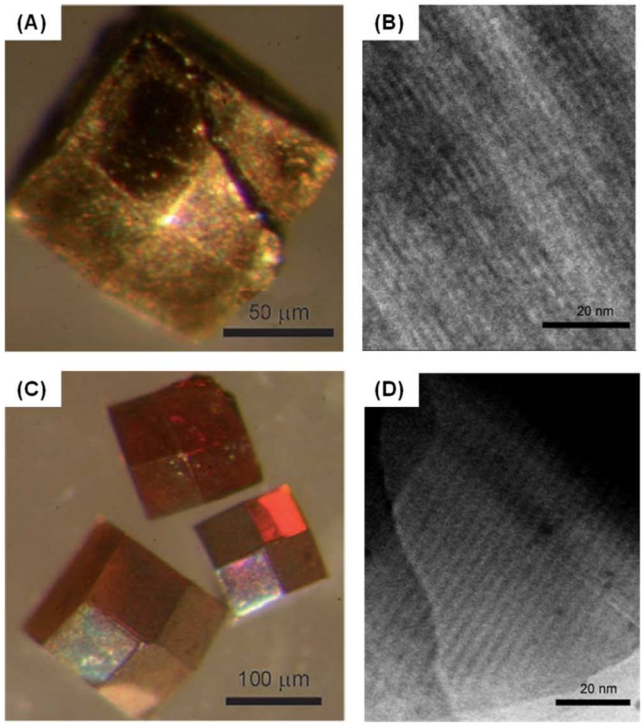

Figure 17. Cross-linked lysozyme crystals were used to direct the synthesis of plasmonic metal nanostructures. Optical and corresponding TEM images of Au nanostructures-doped cross-linked lysozyme crystals (A and B) and Ag nanostructures-doped cross-linked lysozyme crystals (C and D). Reprinted with permission from ref.[114], copyright (2010) John Wiley and Sons.

As mentioned above, the cross-linking and the post-growth of Au nanostructures may cause distortions of or even damages to the single crystal structure of lysozymes. Also, the formation of Au nanostructures via chemical reduction was relative fast, making it quite challenging to perform kinetic studies. To address these issues, Wei et al. developed a novel strategy for *in situ* growth of Au nanoparticles within intact single crystals of lysozyme for the first time (Figure 18).[159] Starting with $ClAuS(CH_2CH_2OH)_2$ (referred to **Au(I)**) as the precursor, they were able to controllably grow Au nanoparticles without using any reducing reagents due to the disproportionation chemistry of **Au(I)**. The formation of Au nanoparticles was slowed down due to the semi-solid nature of protein crystals, making the system amenable to detailed kinetic and mechanism studies. On the other hand, the remained intact single crystals enabled careful structural characterization possible with X-ray crystallography. The time-dependent growth of Au nanoparticles within lysozyme single crystals was monitored by colour change of the crystals and further confirmed by quantitative analysis of Au nanoparticle sizes from TEM images. It clearly showed the gradual growth of

Au nanoparticles within the crystals over time. Further, the 3D distribution of Au nanoparticles within lysozyme crystals was determined by STEM with tomography, validating the encapsulation of Au nanoparticles inside the crystals. More, atomic resolution X-ray crystal structures were obtained. Careful analysis of the crystal structures indicated that certain amino acid residues, such as histidine, played critical roles in directing growth of Au nanoparticles.[159] It also suggested that the growth of Au nanoparticles within lysozyme crystals was a dynamic process and it may involve metal ions transfer, which was supported by later studies.[120, 309] The developed strategy was also applicable to other systems, such as thaumatin protein.[159]

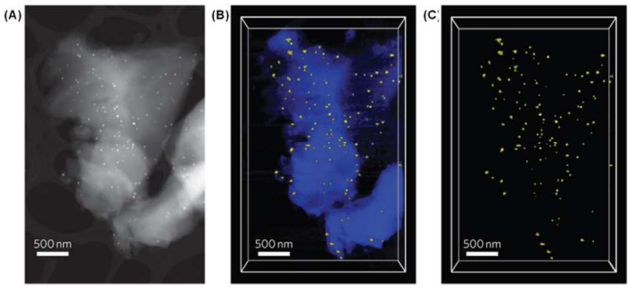

Figure 18. Protein-directed growth of gold nanoparticles within a single crystal of lysozyme. Reprinted with permission from ref.[159], copyright (2011) Nature Publishing Group.

Wei and co-workers also developed an effective way to fine tune the growth of Au nanoparticles within lysozyme single crystals.[159] When using Hg^{2+} ions as an additive, the growth rate was accelerated significantly (Figure 19). Surprisingly, many other divalent metal ions tested did not show such an accelerating effect. This was probably due to the highly specific Ag^{+}-Hg^{2+} metallophilic interaction. When tris(2-carboxyethyl)phosphine (TCEP) was added as an additive, the growth rate was inhibited. The inhibitory effect of TCEP could be caused by the stronger interaction between **Au(I)** and TCEP. Other molecules, such as histidine, could also be used as the inhibitors.[159]

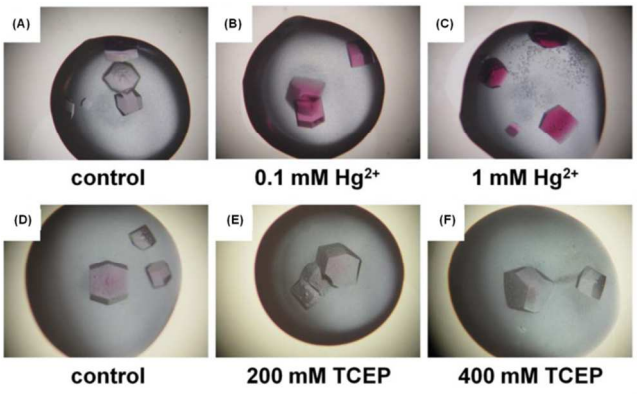

Figure 19. Fine tuning growth of gold nanoparticles within a single crystal of lysozyme. (A-C) accelerating the growth rate by using Hg^{2+} as an additive; (D-E) decelerating the rate of the growth by using TCEP as an additive. Reprinted with permission from ref.[159], copyright (2011) Nature Publishing Group.

Due to the excellent catalytic properties of gold nanomaterials, the catalytic performance of the Au nanoparticles within lysozyme single crystals was also evaluated by Wei et al.[10] Using the reduction of *p*-nitrophenol to *p*-aminophenol by $NaBH_4$ as a model reaction, they showed that the catalytic activities of the Au nanoparticles could be precisely tuned by controlling the growth (thus the sizes) of Au nanoparticles (Figure 20). The relationship between Au nanoparticles' catalytic activity and their size were elucidated. It showed that the Au nanoparticles' catalytic activity initially increased with the increase of nanoparticles' size until the size reached 7.4 nm, after which the activity decreased with increase of nanoparticles' size.[10] It also demonstrated that additives, such as Hg^{2+} and TCEP could be used to fine tune the catalytic activities by controlling the Au nanoparticles' growth. To efficiently recycle the catalysts, the Au nanoparticles-embedded crystals were post cross-linked with glutaraldehyde.[10]

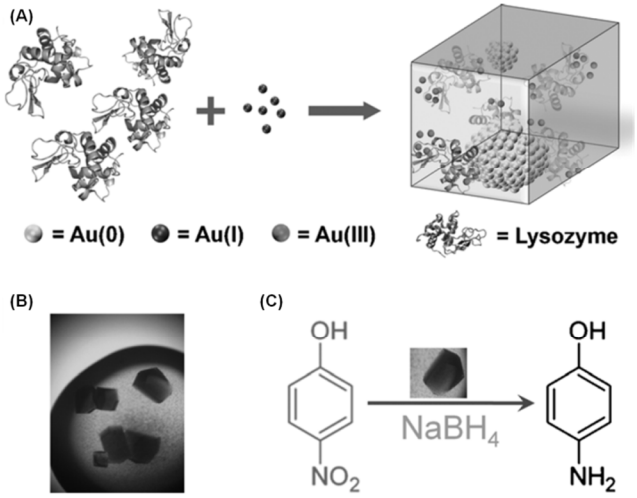

Figure 20. Catalysis of gold nanoparticles within a lysozyme single crystal. Reprinted with permission from ref.[10], copyright (2012) John Wiley and Sons.

Liang et al. employed a slight different approach to synthesis of Au nanoparticles within cross-linked lysozyme crystals.[352] The cross-linked lysozyme crystals were also obtained with glutaraldehyde. Then, $HAuCl_4$ was sequestrated into the crystals by soaking the crystals into $HAuCl_4$ solution. Instead of adding $NaBH_4$ for reduction, NaOH was added into the $HAuCl_4$-soaked crystals at 37 °C for reduction. As discussed above (Section 2.1.1), $HAuCl_4$ could be reduced into Au^0 by certain amino acid residues of lysozyme at basic condition. The as-prepared Au nanoparticles had an average size of 2.2 nm. It further showed that the Au nanoparticles exhibited high activity towards catalytic reduction of *p*-nitrophenol to *p*-aminophenol by $NaBH_4$. More, the Au nanoparticles-doped crystals could be recycled and reused for more than 20 times, showing great potential for practical applications.[352]

3.1.2 Ag

The synthesis of Ag nanostructures within cross-linked lysozyme crystals were also reported by Mann and co-workers.[114] Instead of using a chemical reducing reagent, UV light was applied to reduce the sequestrated silver ions within the cross-linked lysozyme crystals. The formation of Ag nanostructures after *in situ* photoreduction was also followed by the colour change of the crystals and further confirmed by TEM imaging (Figure 17). The

formed Ag nanostructures were also isolated instead of forming continuous nanowires.[354] The transverse and longitudinal plasmonic peaks corresponding to the formed Ag nanostructures were observed at around 412 and 505 nm, respectively.[114] Though the Ag nanostructures-doped crystals exhibited more intact tetragonal morphology compared with the Au nanostructures-doped ones, the X-ray diffraction patterns were deteriorated progressively with the increase of UV irradiation time. These results indicated the proposed methods for synthesis of metal nanostructures could cause the structural distortion of or even damage to the crystal host.

Adopted a similar approach, Ag nanoparticles within cross-linked lysozyme crystals were prepared by Liang and co-workers. The Ag nanoparticles were obtained by reduction of sequestrated $AgNO_3$ with $NaBH_4$.[351] The catalytic reduction of *p*-nitrophenol to *p*-aminophenol by $NaBH_4$ was also demonstrated.

3.2 Others

3.2.1 Quantum dots

Recently, fluorescent semiconductor quantum dots were fabricated within intact single crystals of lysozyme (Figure 21).[162] The CdS quantum dots with red fluorescence were synthesized within single crystals of lysozyme by an *in situ* growth approach. Interestingly, it was found that the CdS quantum dots within the crystals emitted much stronger fluorescence compared with the ones without protein crystals. These results indicated that the protein crystals may provide a unique microenvironment for encapsulated CdS quantum dots with enhanced fluorescence. It also demonstrated that the fluorescence were tuneable. It could be enhanced by the addition of Ag^+ and quenched by Hg^{2+}.[162] The X-ray crystallographic data showed that several amino acid residues, including histidine, participated in the directing formation of CdS quantum dots.

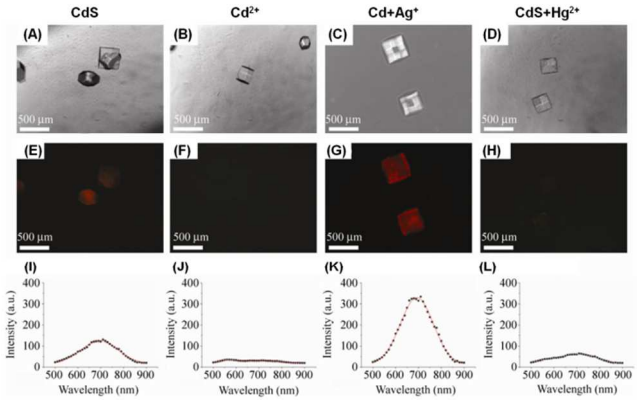

Figure 21. Red fluorescent CdS quantum dots were formed within lysozyme single crystals and the fluorescent properties could be fine-tuned by external chemical stimuli. Bright field (A-D), fluorescence images (E-H), and emission spectra (I-L) of lysozyme single crystals. Reprinted with permission from ref.[162], copyright (2013) Tsinghua University Press and Springer.

3.2.2 Magnetic nanoparticles

It is known that the protein crystalline lattice and thus the sizes and morphologies of the porous pores in protein crystals can be tuned by controlling the crystallization conditions. By exploring this property, Abe et al. synthesized CoPt nanoparticles with different sizes and compositions within cross-linked lysozyme crystals (Figure 22).[169] Orthorhombic, tetragonal, and monoclinic lysozyme crystals were grown with corresponding crystallization buffers. Then the crystals were cross-linked with glutaraldehyde to maintain the lattice structures. After soaking the cross-linked crystals in the buffer solutions containing $CoCl_2$ and K_2PtCl_4, the CoPt nanoparticles were *in situ* formed by chemically reducing the as-soaked Co^{2+} and Pt^{2+} with $NaBH_4$. TEM results clearly showed that the sizes of CoPt nanoparticles were dependent on the pore sizes of the crystals, i.e., large pore could template the formation of large nanoparticles while small pore led to the formation of small nanoparticles (Figure 22).[169] CoPt is among the magnetic materials with high magnetocrystalline anisotropy, therefore their magnetic properties were investigated with a superconducting quantum interference device magnetometer. It was found that the order of the CoPt nanoparticles' coercivity followed the content of Co of the nanoparticles instead of nanoparticles' size, which was consistent with previous report.[169]

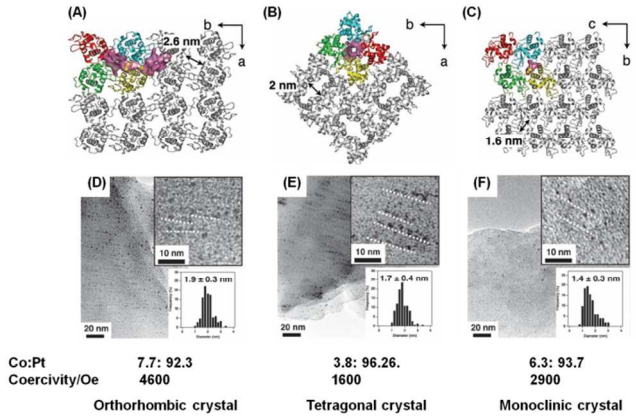

Figure 22. Porous protein crystals as reaction vessels for controlling magnetic properties of CoPt nanoparticles. (A-C) crystal lattice structures of different lysozyme crystals; (D-E) TEM images of CoPt nanoparticles formed in the corresponding cross-linked lysozyme crystals. The Co to Pt ratios and coercivity of the formed CoPt nanoparticles were also listed. Reprinted with permission from ref.[169], copyright (2012) John Wiley and Sons.

X-ray crystallographic structures were also obtained to further understand the mechanism (Figure 23).[169] Both Co^{2+} and Pt^{2+} ions were accumulated within the solvent channels of the crystals. For both orthorhombic and tetragonal lysozyme crystals, the ratio of observed Co to Pt was 1:5, suggesting additional Pt^{2+} ions may be randomly bound to the solvent channels. The crystallographic data suggested that the sizes, compositions, and magnetic properties of CoPt nanoparticles were affected by the number and position of metal ions accumulated.[169] The metal ions translocation was also suggested, which was consistent with previous results.[159, 309]

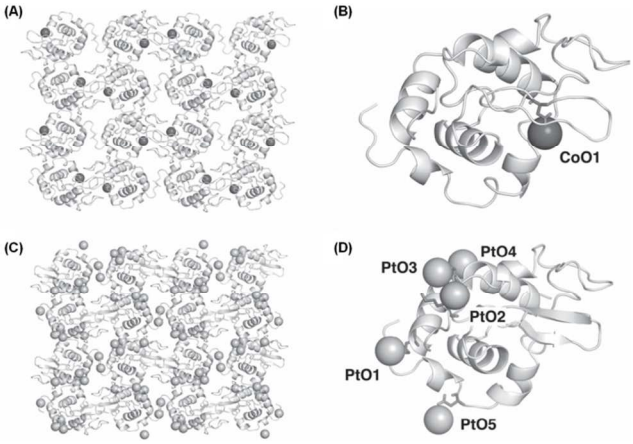

Figure 23. The crystal lattice and molecular structures of cross-linked orthorhombic lysozyme crystal containing Co^{2+} ions (A, B) and Pt^{2+} ions (C, D). Reprinted with permission from ref.[169], copyright (2012) John Wiley and Sons.

Interestingly, when the CoPt nanoparticles were synthesized in lysozyme solution, only aggregates were obtained. The aggregates also showed much lower coercivity compared with the coercivity of CoPt nanoparticles within lysozyme crystals.[169] Such results indicated that the microenvironments and unique structures of lysozyme crystals played critical roles in directing the formation of magnetic CoPt nanoparticles.

3.2.3 Polypyrrole nanostructures

Polypyrrole is a conducting polymer with exceptional biocompatibility and conductive properties, but hard to process due to its intrinsic nature of brittleness and insolubility. To improve the performance of polypyrrole (such as mechanical and electrical properties), Mann and co-workers developed an interesting strategy to template the synthesis and organization of polypyrrole within the solvent channels of cross-linked lysozyme crystals.[164] The glutaraldehyde was used to cross-link the crystals as reported previously. Then the oxidant, ammonium persulfate, was introduced into the channel by soaking. The ammonium persulfate-loaded crystals were then dried and exposed to pyrrole vapour. The partially oxidized polypyrrole was *in situ* formed within the solvent channel after around 24 hours exposure. The as-prepared polypyrrole-doped lysozyme crystals were black/brown in colour. TEM imaging revealed the presence of continuous stripes of 1.8 nm in diameter, which was attributed to the formed polypyrrole (Figure 24). The thickness of stripes matched well with the width of the lysozyme crystals' solvent channels, suggesting the successful templating effect of the cross-linked lysozyme crystals. Though the macroscopic tetragonal morphology was preserved after forming polypyrrole, the crystalline lattice of lysozyme was significantly disrupted because no X-ray diffraction patterns were obtained. Compared with undoped lysozyme crystals, the polypyrrole-doped crystals exhibited measurable conductivity (>10^7 Ωm vs 10^4 Ωm). Note, the conducting mechanism remained to be clarified. More, force-displacement measurements with atomic force microscope revealed that the mechanical plasticity of lysozyme crystals after forming polypyrrole inside was enhanced.[164, 361, 362] The proposed method may be applicable to other conducting materials, such as polyaniline.[164]

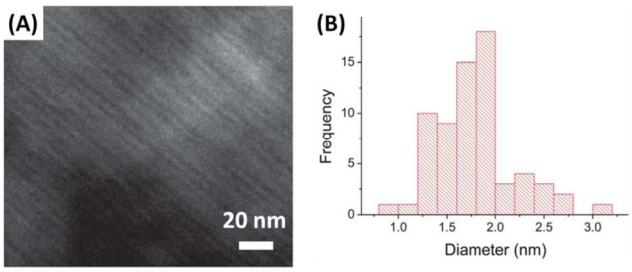

Figure 24. (A) High resolution TEM image of polypyrrole nanostructures formed within the solvent channels of cross-linked lysozyme crystals. (B) The histogram of the diameters of formed the polypyrrole nanostructures. Reprinted with permission from ref.[164], copyright (2012) Royal Society of Chemistry.

4. Conclusions and perspective

This *Feature Article* demonstrates that lysozyme is a valuable model protein to develop synthetic methodologies for various functional nanomaterials, to elucidate the nanomaterials' formation mechanism and protein-nanomaterial interactions, and to explore potential applications (Table S1).

Based on the above discussions, several key points can be summarized as follows: first, proteins and other biomolecules can be used to rationally design and synthesize functional nanomaterials with desired properties for wide applications; second, certain amino acid residues in a protein play critical roles in directing the formation of nanomaterials; third, the unique microenvironments and structures of protein assemblies, such as protein crystals, also play important roles in directing synthesis of functional materials; fourth, combination of advanced techniques such as electron microscopy with tomography and X-ray crystallography from different areas provides a promising opportunity to fully characterize complicated hybrid nanomaterials.

Though substantial progresses have been made in the field of protein directed approaches to functional nanomaterials, several challenges are remained to be addressed.

First, great efforts should be focused on understanding the formation mechanism of functional nanomaterials. For example, even for the extensively studied gold nanoclusters, no exact mechanism was proposed till now.[121, 155, 306, 309] It remains unclear that how the bound gold ions translocate and form final clusters among proteins.[121, 155, 306, 309] On one hand, the ultrasmall size of gold nanoclusters and the presence of protein matrix make it very challenging to obtain structural information by imaging them with TEM. On the other hand, the gold core also affects the MS characterization.[120] High-resolution STEM with tomography, such as STEM with subatomic resolution, may be an alternative approach to get structural information. X-ray crystallography should be another rewarding choice though it is usually very time-consuming.[207] The studies in gas phase will also provide valuable clues and insights to understanding the reaction mechanism in solution phase.[311, 316] Theoretical simulation should not be overlooked because it would be able to predict structural information when combined with experimental results.

Second, the scopes of nanomaterials fabricated should be further explored. The majority of metal nanomaterials discussed

above are noble metal materials. It will be interesting to synthesize other metal materials, such as transitional metal and rare earth nanomaterials, with proteins. Most of the as-prepared nanomaterials are spherical, nanomaterials with other shapes and morphologies should be another focus in the future studies. The design and preparation of multiple functional nanomaterials will be another promising field to be investigated.

Third, most of the model proteins used are lysozyme, BSA, ferritin, heat shock protein etc.[154, 174, 363, 364] Other proteins, especially those with biofunctionalities, should be tested. For example, when the peptide of a small variant of protein A and a Au nanoparticles directing peptide were put together via recombinant protein engineering, the protein chimera could template synthesis of biofunctionalized Au nanoparticles in a one-pot fashion.[158]

The ultimate goal would be rational *de novo* design and synthesis of personalized functional nanomaterials with desired structures and properties based on computation in the future.[365, 366]

Acknowledgements

We would like to thank the National Natural Science Foundation of China (no. 21405081), the Natural Science Foundation of Jiangsu Province (no. BK20130561 and BK20140593), the 985 Program of Nanjing University, the Priority Academic Program Development of Jiangsu Higher Education Institutions (PAPD), and the Thousand Talents Program for Young Researchers for financial support. The authors would like to thank Professor Flavio Maran at University of Padova for the insightful discussions.

Authors

Yubin Ding received his B.S. degree in applied chemistry from Shanxi University in 2008 and Ph.D. degree in applied chemistry from East China University of Science & Technology in 2013. Currently, he is a research assistant professor in Professor Hui Wei's group at Nanjing University. His research interests are focused on design and synthesis of fluorescent probes for biomedical applications.

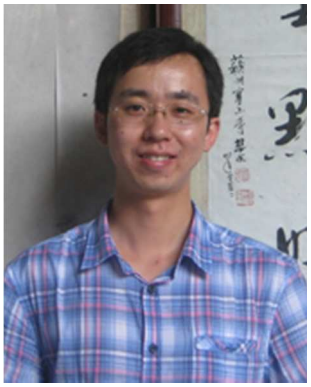

Leilei Shi received his B.S. degree in materials physics from Nanjing University in 2014, where he carried out undergraduate research with Professor Hui Wei. Currently, he is a graduate student in Professor Hui Wei's group at Nanjing University. His research interests are focused on design and synthesis of functional nanomaterials for biomedical applications.

Hui Wei received his B.S. degree in chemistry from Nanjing University in 2003 (advisor: Professor Xinghua Xia) and Ph.D. degree in chemistry from Changchun Institute of Applied Chemistry, Chinese Academy of Sciences in 2008 (advisor: Professor Erkang Wang). After postdoctoral trainings with Professors Yi Lu and Shuming Nie, he joined Nanjing University and started his independent career. Currently, he is a Professor at Nanjing University. His research interests are focused on design and synthesis of functional nanomaterials and development of new methodologies for analytical and biomedical applications.

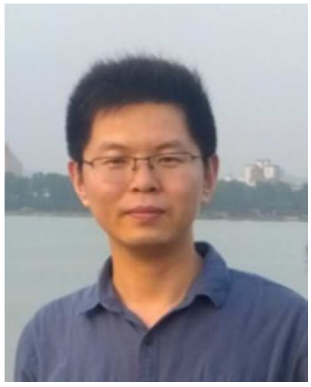

Notes and references

[a] *Department of Biomedical Engineering, College of Engineering and Applied Sciences, Nanjing University, Nanjing, Jiangsu, 210093, China. Fax: +86-25-83594648; Tel: +86-25-83593272; E-mail: weihui@nju.edu.cn*

1. M. Bruchez, M. Moronne, P. Gin, S. Weiss and A. P. Alivisatos, *Science*, 1998, **281**, 2013-2016.
2. A. P. Alivisatos, *Science*, 1996, **271**, 933-937.
3. A. P. Alivisatos, K. P. Johnsson, X. G. Peng, T. E. Wilson, C. J. Loweth, M. P. Bruchez and P. G. Schultz, *Nature*, 1996, **382**, 609-611.
4. P. Alivisatos, *Nat. Biotechnol.*, 2004, **22**, 47-52.
5. W. C. W. Chan and S. M. Nie, *Science*, 1998, **281**, 2016-2018.
6. S. M. Nie and S. R. Emery, *Science*, 1997, **275**, 1102-1106.
7. L. H. Tan, H. Xing and Y. Lu, *Acc. Chem. Res.*, 2014, **47**, 1881-1890.
8. Y. Lu and J. W. Liu, *Acc. Chem. Res.*, 2007, **40**, 315-323.
9. M. Valden, X. Lai and D. W. Goodman, *Science*, 1998, **281**, 1647-1650.
10. H. Wei and Y. Lu, *Chem. Asian J.*, 2012, **7**, 680-683.
11. A. S. Arico, P. Bruce, B. Scrosati, J. M. Tarascon and W. Van Schalkwijk, *Nat. Mater.*, 2005, **4**, 366-377.
12. T. Rueckes, K. Kim, E. Joselevich, G. Y. Tseng, C. L. Cheung and C. M. Lieber, *Science*, 2000, **289**, 94-97.

13. L. Zhang, H. X. Chang, A. Hirata, H. K. Wu, Q. K. Xue and M. W. Chen, *ACS Nano*, 2013, **7**, 4595-4600.
14. H. Wei, B. L. Li, J. Li, S. J. Dong and E. K. Wang, *Nanotechnology*, 2008, **19**, 095501.
15. R. Elghanian, J. J. Storhoff, R. C. Mucic, R. L. Letsinger and C. A. Mirkin, *Science*, 1997, **277**, 1078-1081.
16. C. M. Niemeyer, *Angew. Chem. Int. Ed.*, 2001, **40**, 4128-4158.
17. E. Katz and I. Willner, *Angew. Chem. Int. Ed.*, 2004, **43**, 6042-6108.
18. M. C. Daniel and D. Astruc, *Chem. Rev.*, 2004, **104**, 293-346.
19. N. L. Rosi and C. A. Mirkin, *Chem. Rev.*, 2005, **105**, 1547-1562.
20. H. Wei, B. L. Li, J. Li, E. K. Wang and S. J. Dong, *Chem. Commun.*, 2007, 3735-3737.
21. Y. Wang, H. Wei, B. Li, W. Ren, S. Guo, S. Dong and E. Wang, *Chem. Commun.*, 2007, 5220-5222.
22. H. Wei, Y. Du, J. Z. Kang and E. K. Wang, *Electrochem. Commun.*, 2007, **9**, 1474-1479.
23. C. L. Guo, Y. H. Song, H. Wei, P. C. Li, L. Wang, L. L. Sun, Y. J. Sun and Z. Li, *Anal. Bioanal. Chem.*, 2007, **389**, 527-532.
24. G. Wei, L. Wang, L. L. Sun, Y. H. Song, Y. J. Sun, C. L. Guo, T. Yang and Z. Li, *J. Phys. Chem. C*, 2007, **111**, 1976-1982.
25. H. Wei and E. Wang, *Anal. Chem.*, 2008, **80**, 2250-2254.
26. H. Wei, C. G. Chen, B. Y. Han and E. K. Wang, *Anal. Chem.*, 2008, **80**, 7051-7055.
27. L. L. Sun, Y. H. Song, L. Wang, C. L. Guo, Y. J. Sun, Z. L. Liu and Z. Li, *J. Phys. Chem. C*, 2008, **112**, 1415-1422.
28. Z. Z. Lv, H. Wei, B. L. Li and E. K. Wang, *Analyst*, 2009, **134**, 1647-1651.
29. F. G. Xu, K. Cui, Y. J. Sun, C. L. Guo, Z. L. Liu, Y. Zhang, Y. Shi and Z. Li, *Talanta*, 2010, **82**, 1845-1852.
30. L. B. Zhang, H. Wei, J. Li, T. Li, D. Li, Y. H. Li and E. K. Wang, *Biosens. Bioelectron.*, 2010, **25**, 1897-1901.
31. Y. Zhang, F. G. Xu, Y. J. Sun, C. L. Guo, K. Cui, Y. Shi, Z. W. Wen and Z. Li, *Chem. Eur. J.*, 2010, **16**, 9248-9256.
32. Z. L. Liu, B. Zhao, Y. Shi, C. L. Guo, H. B. Yang and Z. Li, *Talanta*, 2010, **81**, 1650-1654.
33. H. Wei and E. K. Wang, *Chem. Soc. Rev.*, 2013, **42**, 6060-6093.
34. S. H. Gao, F. Y. Liu, B. T. Zhang, Y. J. Wang, H. M. Zhang and Z. X. Wang, *Chinese J. Anal. Chem.* , 2013, **41**, 811-816.
35. Q. H. Guo, J. S. Huang and T. Y. You, *Chinese J. Anal. Chem.* , 2013, **41**, 210-214.
36. S. J. Guo and E. K. Wang, *Acc. Chem. Res.*, 2011, **44**, 491-500.
37. C. X. Li, J. Adamcik and R. Mezzenga, *Nat. Nanotechnol.*, 2012, **7**, 421-427.
38. Y. A. Yuan, X. X. He, H. Shi, K. M. Wang, X. Wu and X. Q. Huo, *Chem. J. Chinese Univ.*, 2010, **31**, 2167-2172.
39. H. Zhong, H. P. Xu and H. Zhang, *Chinese J. Anal. Chem.* , 2014, **42**, 475-481.
40. L. Shang, K. Nienhaus and G. U. Nienhaus, *J. Nanobiotechnol.*, 2014, **12**, 11.
41. L. Treuel, S. Brandholt, P. Maffre, S. Wiegele, L. Shang and G. U. Nienhaus, *ACS Nano*, 2014, **8**, 503-513.
42. L. Shang and S. J. Dong, *Anal. Chem.*, 2009, **81**, 1465-1470.
43. L. Shang, J. Y. Yin, J. Li, L. H. Jin and S. J. Dong, *Biosens. Bioelectron.*, 2009, **25**, 269-274.
44. S. Mura, G. Greppi, P. Innocenzi, M. Piccinini, C. Figus, M. L. Marongiu, C. L. Guo and J. Irudayaraj, *J. Raman Spectrosc.*, 2013, **44**, 35-40.
45. C. Wang, X. Q. Hao, M. Wang, C. L. Guo, B. Q. Xu, E. N. Tan, Y. Y. Zhang, Y. H. Yu, Z. Y. Li, H. B. Yang, M. P. Song and X. P. Li, *Chem. Sci.*, 2014, **5**, 1221-1226.
46. J. F. Zhou, S. Samanta, C. L. Guo, J. Locklin and B. Q. Xu, *Nanoscale*, 2013, **5**, 5715-5719.
47. Z. L. Liu, B. Zhao, C. L. Guo, Y. J. Sun, Y. Shi, H. B. Yang and Z. Li, *J. Colloid Interf. Sci.*, 2010, **351**, 233-238.
48. F. G. Xu, C. L. Guo, Y. J. Sun, Z. L. Liu, Y. Zhang and Z. Li, *Colloid. Surface. A.*, 2010, **353**, 125-131.
49. L. L. Sun, Y. J. Sun, F. G. Xu, Y. Zhang, T. Yang, C. L. Guo, Z. L. Liu and Z. Li, *Nanotechnology*, 2009, **20**, 125502.
50. Z. L. Liu, B. Zhao, C. L. Guo, Y. J. Sun, F. G. Xu, H. B. Yang and Z. Li, *J. Phys. Chem. C*, 2009, **113**, 16766-16771.
51. L. Wang, G. Wei, C. L. Guo, L. L. Sun, Y. J. Sun, Y. G. Song, T. Yang and Z. Li, *Colloid. Surface. A.*, 2008, **312**, 148-153.
52. L. L. Sun, Y. H. Song, G. Wei, L. Wang, C. L. Guo, Y. J. Sun and Z. Li, *Chem. Lett.*, 2007, **36**, 142-143.
53. L. Wang, G. Wei, L. L. Sun, Z. G. Liu, Y. H. Song, T. Yang, Y. J. Sun, C. L. Guo and Z. Li, *Nanotechnology*, 2006, **17**, 2907-2912.
54. L. L. Sun, L. Wang, Y. H. Song, C. L. Guo, Y. J. Sun, C. Y. Peng, Z. L. Liu and Z. Li, *Appl. Surf. Sci.*, 2008, **254**, 2581-2587.
55. L. Wang, Y. H. Song, L. L. Sun, C. L. Guo, Y. J. Sun and Z. Li, *Mater. Lett.*, 2008, **62**, 4124-4126.
56. Y. H. Song, Z. Li, Z. G. Liu, G. Wei, L. Wang, L. L. Sun, C. L. Guo, Y. J. Sun and T. Yang, *J. Phys. Chem. B*, 2006, **110**, 10792-10798.
57. Y. Du, H. Wei, J. Z. Kang, J. L. Yan, X. B. Yin, X. R. Yang and E. K. Wang, *Anal. Chem.*, 2005, **77**, 7993-7997.
58. B. L. Li, Y. L. Wang, H. Wei and S. J. Dong, *Biosens. Bioelectron.*, 2008, **23**, 965-970.
59. L. Y. Fang, Z. Z. Lv, H. Wei and E. Wang, *Anal. Chim. Acta*, 2008, **628**, 80-86.
60. J. Li, Y. H. Xu, H. Wei, T. Huo and E. K. Wang, *Anal. Chem.*, 2007, **79**, 5439-5443.
61. J. Li, M. H. Huang, X. Q. Liu, H. Wei, Y. H. Xu, G. B. Xu and E. K. Wang, *Analyst*, 2007, **132**, 687-691.
62. J. G. Bai, H. Wei, B. L. Li, L. H. Song, L. Y. Fang, Z. Z. Lv, W. H. Zhou and E. K. Wang, *Chem. Asian J.*, 2008, **3**, 1935-1941.
63. H. Wei, J. Y. Yin and E. Wang, *Anal. Chem.*, 2008, **80**, 5635-5639.
64. H. Wei, Y. Du, J. Z. Kang, G. B. Xu and E. K. Wang, *Chin. J. Chem.*, 2007, **25**, 159-163.
65. X. H. Gao, Y. Y. Cui, R. M. Levenson, L. W. K. Chung and S. M. Nie, *Nat. Biotechnol.*, 2004, **22**, 969-976.
66. M. Y. Han, X. H. Gao, J. Z. Su and S. Nie, *Nat. Biotechnol.*, 2001, **19**, 631-635.
67. X. M. Qian, X. H. Peng, D. O. Ansari, Q. Yin-Goen, G. Z. Chen, D. M. Shin, L. Yang, A. N. Young, M. D. Wang and S. M. Nie, *Nat. Biotechnol.*, 2008, **26**, 83-90.
68. J. Kong, N. R. Franklin, C. W. Zhou, M. G. Chapline, S. Peng, K. J. Cho and H. J. Dai, *Science*, 2000, **287**, 622-625.
69. Y. N. Xia, P. D. Yang, Y. G. Sun, Y. Y. Wu, B. Mayers, B. Gates, Y. D. Yin, F. Kim and Y. Q. Yan, *Adv. Mater.*, 2003, **15**, 353-389.
70. Y. Cui, Q. Q. Wei, H. K. Park and C. M. Lieber, *Science*, 2001, **293**, 1289-1292.
71. Y. Huang, X. F. Duan, Y. Cui, L. J. Lauhon, K. H. Kim and C. M. Lieber, *Science*, 2001, **294**, 1313-1317.
72. Z. N. Bao, J. A. Rogers and H. E. Katz, *J. Mater. Chem.*, 1999, **9**, 1895-1904.
73. S. H. Sun, C. B. Murray, D. Weller, L. Folks and A. Moser, *Science*, 2000, **287**, 1989-1992.
74. C. B. Murray, D. J. Norris and M. G. Bawendi, *J. Am. Chem. Soc.*, 1993, **115**, 8706-8715.
75. C. J. Murphy, T. K. San, A. M. Gole, C. J. Orendorff, J. X. Gao, L. Gou, S. E. Hunyadi and T. Li, *J. Phys. Chem. B*, 2005, **109**, 13857-13870.
76. P. K. Jain, X. H. Huang, I. H. El-Sayed and M. A. El-Sayed, *Acc. Chem. Res.*, 2008, **41**, 1578-1586.
77. A. M. Smith, H. W. Duan, A. M. Mohs and S. M. Nie, *Adv. Drug. Deliver. Rev.*, 2008, **60**, 1226-1240.
78. K. Saha, S. S. Agasti, C. Kim, X. N. Li and V. M. Rotello, *Chem. Rev.*, 2012, **112**, 2739-2779.
79. Z. Y. Tang, N. A. Kotov and M. Giersig, *Science*, 2002, **297**, 237-240.
80. Z. Y. Tang, Y. Wang, P. Podsiadlo and N. A. Kotov, *Adv. Mater.*, 2006, **18**, 3203-3224.
81. L. X. Zhang, P. C. Li, X. H. Liu, L. W. Du and E. Wang, *Adv. Mater.*, 2007, **19**, 4279-4283.
82. W. Yang, X. L. Wang, F. Yang, C. Yang and X. R. Yang, *Adv. Mater.*, 2008, **20**, 2579-2587.

83. Y. Jiang, H. Zhao, Y. Q. Lin, N. N. Zhu, Y. R. Ma and L. Q. Mao, *Angew. Chem. Int. Ed.*, 2010, **49**, 4800-4804.
84. Y. Jiang, H. Zhao, N. N. Zhu, Y. Q. Lin, P. Yu and L. Q. Mao, *Angew. Chem. Int. Ed.*, 2008, **47**, 8601-8604.
85. K. L. Ai, Y. L. Liu and L. H. Lu, *J. Am. Chem. Soc.*, 2009, **131**, 9496-9497.
86. L. L. Li, Q. Yin, J. J. Cheng and Y. Lu, *Adv. Healthcare Mater.*, 2012, **1**, 567-572.
87. L. L. Li, R. B. Zhang, L. L. Yin, K. Z. Zheng, W. P. Qin, P. R. Selvin and Y. Lu, *Angew. Chem. Int. Ed.*, 2012, **51**, 6121-6125.
88. L. L. Li, P. W. Wu, K. Hwang and Y. Lu, *J. Am. Chem. Soc.*, 2013, **135**, 2411-2414.
89. L. L. Li, M. Y. Xie, J. Wang, X. Y. Li, C. Wang, Q. Yuan, D. W. Pang, Y. Lu and W. H. Tan, *Chem. Commun.*, 2013, **49**, 5823-5825.
90. Y. D. Jin, D. Cahen, N. Friedman and M. Sheves, *Angew. Chem. Int. Ed.*, 2006, **45**, 6325-6328.
91. E. M. Saurer, R. M. Flessner, S. P. Sullivan, M. R. Prausnitz and D. M. Lynn, *Biomacromolecules*, 2010, **11**, 3136-3143.
92. S. K. M. Nalluri, C. Berdugo, N. Javid, P. Frederix and R. V. Ulijn, *Angew. Chem. Int. Ed.*, 2014, **53**, 5882-5887.
93. L. Kabalah-Amitai, B. Mayzel, Y. Kauffmann, A. N. Fitch, L. Bloch, P. Gilbert and B. Pokroy, *Science*, 2013, **340**, 454-457.
94. M. Reches and E. Gazit, *Science*, 2003, **300**, 625-627.
95. H. Wei, B. L. Li, Y. Du, S. J. Dong and E. Wang, *Chem. Mater.*, 2007, **19**, 2987-2993.
96. H. Wei and E. K. Wang, *Nanotechnology*, 2007, **18**, 295603.
97. H. Wei, J. Li, Y. L. Wang and E. K. Wang, *Nanotechnology*, 2007, **18**, 175610.
98. C. L. Guo, Y. H. Song, L. Wang, L. L. Sun, Y. J. Sun, C. Y. Peng, Z. L. Liu, T. Yang and Z. Li, *J. Phys. Chem. B*, 2008, **112**, 1022-1027.
99. C. L. Guo, G. P. Li, Z. L. Liu, L. L. Sun, Y. J. Sun, F. G. Xu, Y. Zhang, T. Yang and Z. Li, *Chemphyschem*, 2009, **10**, 1624-1629.
100. C. L. Guo, Z. L. Liu, F. G. Xu, L. L. Sun, Y. J. Sun, T. Yang and Z. Li, *J. Phys. Chem. B*, 2009, **113**, 6068-6073.
101. Z. D. Wang, J. Q. Zhang, J. M. Ekman, P. J. A. Kenis and Y. Lu, *Nano Lett.*, 2010, **10**, 1886-1891.
102. C. Y. Chiu, Y. J. Li, L. Y. Ruan, X. C. Ye, C. B. Murray and Y. Huang, *Nat. Chem.*, 2011, **3**, 393-399.
103. G. Tikhomirov, S. Hoogland, P. E. Lee, A. Fischer, E. H. Sargent and S. O. Kelley, *Nat. Nanotechnol.*, 2011, **6**, 485-490.
104. Z. Zhao, E. L. Jacovetty, Y. Liu and H. Yan, *Angew. Chem. Int. Ed.*, 2011, **50**, 2041-2044.
105. D. K. Lim, K. S. Jeon, J. H. Hwang, H. Kim, S. Kwon, Y. D. Suh and J. M. Nam, *Nat. Nanotechnol.*, 2011, **6**, 452-460.
106. Z. D. Wang, L. H. Tang, L. H. Tan, J. H. Li and Y. Lu, *Angew. Chem. Int. Ed.*, 2012, **51**, 9078-9082.
107. L. Y. T. Chou, K. Zagorovsky and W. C. W. Chan, *Nat. Nanotechnol.*, 2014, **9**, 148-155.
108. A. L. Margolin and M. A. Navia, *Angew. Chem. Int. Ed.*, 2001, **40**, 2204-2222.
109. M. L. Flenniken, D. A. Willits, S. Brumfield, M. J. Young and T. Douglas, *Nano Lett.*, 2003, **3**, 1573-1576.
110. J. C. Falkner, M. E. Turner, J. K. Bosworth, T. J. Trentler, J. E. Johnson, T. W. Lin and V. L. Colvin, *J. Am. Chem. Soc.*, 2005, **127**, 5274-5275.
111. C. A. Butts, J. Swift, S. G. Kang, L. Di Costanzo, D. W. Christianson, J. G. Saven and I. J. Dmochowski, *Biochemistry*, 2008, **47**, 12729-12739.
112. M. Suzuki, M. Abe, T. Ueno, S. Abe, T. Goto, Y. Toda, T. Akita, Y. Yamadae and Y. Watanabe, *Chem. Commun.*, 2009, 4871-4873.
113. P. L. Xavier, K. Chaudhari, P. K. Verma, S. K. Pal and T. Pradeep, *Nanoscale*, 2010, **2**, 2769-2776.
114. M. Guli, E. M. Lambert, M. Li and S. Mann, *Angew. Chem. Int. Ed.*, 2010, **49**, 520-523.
115. A. Mathew, P. R. Sajanlal and T. Pradeep, *J. Mater. Chem.*, 2011, **21**, 11205-11212.
116. H. W. Li, K. L. Ai and Y. Q. Wu, *Chem. Commun.*, 2011, **47**, 9852-9854.
117. C. L. Guo and J. Irudayaraj, *Anal. Chem.*, 2011, **83**, 2883-2889.
118. C. Guo, B. Book-Newell and J. Irudayaraj, *Chem. Commun.*, 2011, **47**, 12658-12660.
119. D. C. Bassett, L. M. Grover, F. A. Muller, M. D. McKee and J. E. Barralet, *Adv. Funct. Mater.*, 2011, **21**, 2968-2977.
120. K. Chaudhari, P. L. Xavier and T. Pradeep, *ACS Nano*, 2011, **5**, 8816-8827.
121. T. H. Chen and W. L. Tseng, *Small*, 2012, **8**, 1912-1919.
122. H. Y. Li, H. L. Xin, D. A. Muller and L. A. Estroff, *Science*, 2009, **326**, 1244-1247.
123. V. Berry, A. Gole, S. Kundu, C. J. Murphy and R. F. Saraf, *J. Am. Chem. Soc.*, 2005, **127**, 17600-17601.
124. T. J. Park, S. Y. Lee, N. S. Heo and T. S. Seo, *Angew. Chem. Int. Ed.*, 2010, **49**, 7019-7024.
125. K. T. Nam, D. W. Kim, P. J. Yoo, C. Y. Chiang, N. Meethong, P. T. Hammond, Y. M. Chiang and A. M. Belcher, *Science*, 2006, **312**, 885-888.
126. Y. J. Lee, H. Yi, W. J. Kim, K. Kang, D. S. Yun, M. S. Strano, G. Ceder and A. M. Belcher, *Science*, 2009, **324**, 1051-1055.
127. H. F. Bao, Z. S. Lu, X. Q. Cui, Y. Qiao, J. Guo, J. M. Anderson and C. M. Li, *Acta Biomater.*, 2010, **6**, 3534-3541.
128. S. R. Sturzenbaum, M. Hockner, A. Panneerselvam, J. Levitt, J. S. Bouillard, S. Taniguchi, L. A. Dailey, R. A. Khanbeigi, E. V. Rosca, M. Thanou, K. Suhling, A. V. Zayats and M. Green, *Nat. Nanotechnol.*, 2013, **8**, 57-60.
129. J. L. Wang, G. Zhang, Q. W. Li, H. Jiang, C. Y. Liu, C. Amatore and X. M. Wang, *Sci. Rep.*, 2013, **3**, 1157.
130. S. P. Gao, D. H. Chen, Q. W. Li, J. Ye, H. Jiang, C. Amatore and X. M. Wang, *Sci. Rep.*, 2014, **4**, 4384.
131. G. L. Liu, Q. Feng, X. Y. Mu, W. J. Zheng, T. F. Chen, L. Qib and D. Li, *J. Mater. Chem. B*, 2013, **1**, 2128-2131.
132. G. Q. Wang, H. Mitomo, Y. Matsuo, N. Shimamoto, K. Niikura and K. Ijiro, *J. Mater. Chem. B*, 2013, **1**, 5899-5907.
133. M. Wysokowski, M. Motylenko, H. Stocker, V. V. Bazhenov, E. Langer, A. Dobrowolska, K. Czaczyk, R. Galli, A. L. Stelling, T. Behm, L. Klapiszewski, D. Ambrozewicz, M. Nowacka, S. L. Molodtsov, B. Abendroth, D. C. Meyer, K. J. Kurzydlowski, T. Jesionowski and H. Ehrlich, *J. Mater. Chem. B*, 2013, **1**, 6469-6476.
134. Z. Zhen, W. Tang, C. Guo, H. Chen, X. Lin, G. Liu, B. Fei, X. Chen, B. Xu and J. Xie, *ACS Nano*, 2013, **7**, 6988-6996.
135. Z. X. Zhou, W. Wei, Y. J. Zhang and S. Q. Liu, *J. Mater. Chem. B*, 2013, **1**, 2851-2858.
136. B. Soptei, L. N. Nagy, P. Baranyai, I. Szabo, G. Mezo, F. Hudecz and A. Bota, *Gold Bull.*, 2013, **46**, 195-203.
137. X. H. Liu, L. X. Zhang, Y. L. Wang, C. L. Guo and E. K. Wang, *Cryst. Growth Des.*, 2008, **8**, 759-762.
138. Y. J. Sun, L. L. Sun, F. G. Xu, C. L. Guo, Z. L. Liu, Y. Zhang, T. Yang and Z. Li, *Appl. Surf. Sci.*, 2009, **255**, 6814-6818.
139. Y. J. Sun, L. L. Sun, B. H. Zhang, F. G. Xu, Z. L. Liu, C. L. Guo, Y. Zhang and Z. Li, *Talanta*, 2009, **79**, 562-569.
140. L. L. Sun, Y. H. Song, L. Wang, Y. J. Sun, C. L. Guo, Z. L. Liu and Z. Li, *J. Nanosci. Nanotechnol.*, 2008, **8**, 4415-4423.
141. Y. J. Sun, G. Wei, Y. H. Song, L. Wang, L. L. Sun, C. L. Guo, T. Yang and Z. Li, *Nanotechnology*, 2008, **19**, 115604.
142. Y. H. Song, C. L. Guo, L. L. Sun, G. Wei, C. Y. Peng, L. Wang, Y. J. Sun and Z. Li, *J. Phys. Chem. B*, 2007, **111**, 461-468.
143. Y. J. Sun, L. Wang, L. L. Sun, C. L. Guo, T. Yang, Z. L. Liu, F. G. Xu and Z. Li, *J. Chem. Phys.*, 2008, **128**, 074704.
144. W. Shenton, T. Douglas, M. Young, G. Stubbs and S. Mann, *Adv. Mater.*, 1999, **11**, 253-256.
145. T. Ueno, M. Suzuki, T. Goto, T. Matsumoto, K. Nagayama and Y. Watanabe, *Angew. Chem. Int. Ed.*, 2004, **43**, 2527-2530.
146. N. Goswami, A. Giri, S. Kar, M. S. Bootharaju, R. John, P. L. Xavier, T. Pradeep and S. K. Pal, *Small*, 2012, **8**, 3175-3184.
147. M. Reches and E. Gazit, *Nat. Nanotechnol.*, 2006, **1**, 195-200.
148. L. Fabris, S. Antonello, L. Armelao, R. L. Donkers, F. Polo, C. Toniolo and F. Maran, *J. Am. Chem. Soc.*, 2006, **128**, 326-336.

149. I. Ron, I. Pecht, M. Sheves and D. Cahen, *Acc. Chem. Res.*, 2010, **43**, 945-953.
150. A. Gitelman and H. Rapaport, *Langmuir*, 2014, **30**, 4716-4724.
151. A. Brif, G. Ankonina, C. Drathen and B. Pokroy, *Adv. Mater.*, 2014, **26**, 477-481.
152. G. Pieters, C. Pezzato and L. J. Prins, *J. Am. Chem. Soc.*, 2012, **134**, 15289-15292.
153. M. Ritenberg, E. Beilis, A. Ilovitsh, Z. Barkai, A. Shahmoon, S. Richter, Z. Zalevsky and R. Jelinek, *Sci. Rep.*, 2014, **4**, 3666.
154. J. P. Xie, Y. G. Zheng and J. Y. Ying, *J. Am. Chem. Soc.*, 2009, **131**, 888-889.
155. H. Wei, Z. D. Wang, L. M. Yang, S. L. Tian, C. J. Hou and Y. Lu, *Analyst*, 2010, **135**, 1406-1410.
156. J. P. Xie, Y. G. Zheng and J. Y. Ying, *Chem. Commun.*, 2010, **46**, 961-963.
157. C. L. Liu, H. T. Wu, Y. H. Hsiao, C. W. Lai, C. W. Shih, Y. K. Peng, K. C. Tang, H. W. Chang, Y. C. Chien, J. K. Hsiao, J. T. Cheng and P. T. Chou, *Angew. Chem. Int. Ed.*, 2011, **50**, 7056-7060.
158. M. Colombo, S. Mazzucchelli, V. Collico, S. Avvakumova, L. Pandolfi, F. Corsi, F. Porta and D. Prosperi, *Angew. Chem. Int. Ed.*, 2012, **51**, 9272-9275.
159. H. Wei, Z. D. Wang, J. O. Zhang, S. House, Y. G. Gao, L. M. Yang, H. Robinson, L. H. Tan, H. Xing, C. J. Hou, I. M. Robertson, J. M. Zuo and Y. Lu, *Nat. Nanotechnol.*, 2011, **6**, 93-97.
160. Z. Xu, X. W. Liu, Y. S. Ma and H. W. Gao, *Environ. Sci. Pollut. Res.*, 2010, **17**, 798-806.
161. H. R. Luckarift, M. B. Dickerson, K. H. Sandhage and J. C. Spain, *Small*, 2006, **2**, 640-643.
162. H. Wei, S. House, J. J. X. Wu, J. Zhang, Z. D. Wang, Y. He, E. J. Gao, Y. G. Gao, H. Robinson, W. Li, J. M. Zuo, I. M. Robertson and Y. Lu, *Nano Res.*, 2013, **6**, 627-634.
163. L. Ma, H. Y. Liu, Z. C. Zhu, H. L. Wang, X. Y. Xu, N. Na and O. Y. Jin, *J. Mater. Chem. A*, 2013, **1**, 15082-15088.
164. M. W. England, E. M. Lambert, M. Li, L. Turyanska, A. J. Patil and S. Mann, *Nanoscale*, 2012, **4**, 6710-6713.
165. T. Shiomi, T. Tsunoda, A. Kawai, F. Mizukami and K. Sakaguchi, *Chem. Mater.*, 2007, **19**, 4486-4493.
166. B. H. San, S. Lee, S. H. Moh, J. G. Park, J. H. Lee, H. Y. Hwang and K. K. Kim, *J. Mater. Chem. B*, 2013, **1**, 1453-1460.
167. R. E. Canfield, *J. Biol. Chem.*, 1963, **238**, 2698-2707.
168. M. J. Panzner, S. M. Bilinovich, W. J. Youngs and T. C. Leeper, *Chem. Commun.*, 2011, **47**, 12479-12481.
169. S. Abe, M. Tsujimoto, K. Yoneda, M. Ohba, T. Hikage, M. Takano, S. Kitagawa and T. Ueno, *Small*, 2012, **8**, 1314-1319.
170. C. Liu, D. Yang, Y. Jiao, Y. Tian, Y. G. Wang and Z. Y. Jiang, *ACS Appl. Mater. Interfaces*, 2013, **5**, 3824-3832.
171. T. Yang, Z. Li, L. Wang, C. L. Guo and Y. J. Sun, *Langmuir*, 2007, **23**, 10533-10538.
172. T. Y. Zhou, Y. H. Huang, W. B. Li, Z. M. Cai, F. Luo, C. J. Yang and X. Chen, *Nanoscale*, 2012, **4**, 5312-5315.
173. M. Sarikaya, C. Tamerler, A. K. Y. Jen, K. Schulten and F. Baneyx, *Nat. Mater.*, 2003, **2**, 577-585.
174. M. Uchida, M. T. Klem, M. Allen, P. Suci, M. Flenniken, E. Gillitzer, Z. Varpness, L. O. Liepold, M. Young and T. Douglas, *Adv. Mater.*, 2007, **19**, 1025-1042.
175. M. B. Dickerson, K. H. Sandhage and R. R. Naik, *Chem. Rev.*, 2008, **108**, 4935-4978.
176. R. V. Ulijn and A. M. Smith, *Chem. Soc. Rev.*, 2008, **37**, 664-675.
177. L. Berti and G. A. Burley, *Nat. Nanotechnol.*, 2008, **3**, 81-87.
178. Z. D. Wang and Y. Lu, *J. Mater. Chem.*, 2009, **19**, 1788-1798.
179. R. de la Rica and H. Matsui, *Chem. Soc. Rev.*, 2010, **39**, 3499-3509.
180. J. M. Slocik and R. R. Naik, *Chem. Soc. Rev.*, 2010, **39**, 3454-3463.
181. C. L. Chen and N. L. Rosi, *Angew. Chem. Int. Ed.*, 2010, **49**, 1924-1942.
182. M. R. Jones, K. D. Osberg, R. J. Macfarlane, M. R. Langille and C. A. Mirkin, *Chem. Rev.*, 2011, **111**, 3736-3827.
183. J. M. Galloway and S. S. Staniland, *J. Mater. Chem.*, 2012, **22**, 12423-12434.
184. D. M. Chevrier, A. Chatt and P. Zhang, *J. Nanophotonics*, 2012, **6**, 064504.
185. V. Bonacic-Koutecky, A. Kulesza, L. Gell, R. Mitric, R. Antoine, F. Bertorelle, R. Hamouda, D. Rayane, M. Broyer, T. Tabarin and P. Dugourd, *Phys. Chem. Chem. Phys.*, 2012, **14**, 9282-9290.
186. S. T. Yang, Y. Liu, Y. W. Wang and A. N. Cao, *Small*, 2013, **9**, 1635-1653.
187. C. Y. Chiu, L. Y. Ruan and Y. Huang, *Chem. Soc. Rev.*, 2013, **42**, 2512-2527.
188. K. E. Sapsford, W. R. Algar, L. Berti, K. B. Gemmill, B. J. Casey, E. Oh, M. H. Stewart and I. L. Medintz, *Chem. Rev.*, 2013, **113**, 1904-2074.
189. N. J. M. Sanghamitra and T. Ueno, *Chem. Commun.*, 2013, **49**, 4114-4126.
190. T. Ueno, *Chem. Eur. J.*, 2013, **19**, 9096-9102.
191. E. Gazit, *Chem. Soc. Rev.*, 2007, **36**, 1263-1269.
192. T. P. J. Knowles, T. W. Oppenheim, A. K. Buell, D. Y. Chirgadze and M. E. Welland, *Nat. Nanotechnol.*, 2010, **5**, 204-207.
193. J. B. Xie, M. Qin, Y. Cao and W. Wang, *Proteins*, 2011, **79**, 2505-2516.
194. J. B. Xie, Y. Cao, H. Pan, M. Qin, Z. Q. Yan, X. Xiong and W. Wang, *Proteins*, 2012, **80**, 2501-2513.
195. F. Cavalieri, M. Ashokkumar, F. Grieser and F. Caruso, *Langmuir*, 2008, **24**, 10078-10083.
196. M. F. Zhou, T. S. H. Leong, S. Melino, F. Cavalieri, S. Kentish and M. Ashokkumar, *Ultrason. Sonochem.*, 2010, **17**, 333-337.
197. Q.-Q. Gai, F. Qu, Z.-J. Liu, R.-J. Dai and Y.-K. Zhang, *J. Chromatogr. A*, 2010, **1217**, 5035-5042.
198. G. Fu, H. He, Z. Chai, H. Chen, J. Kong, Y. Wang and Y. Jiang, *Analytical Chemistry*, 2011, **83**, 1431-1436.
199. Z. Lin, Z. Xia, J. Zheng, D. Zheng, L. Zhang, H. Yang and G. Chen, *J. Mater. Chem.*, 2012, **22**, 17914-17922.
200. G. Pan, Q. Guo, C. Cao, H. Yang and B. Li, *Soft Matter*, 2013, **9**, 3840-3850.
201. Z. Lin, Y. Lin, X. Sun, H. Yang, L. Zhang and G. Chen, *J. Chromatogr. A*, 2013, **1284**, 8-16.
202. X. Li, B. Zhang, L. Tian, W. Li, T. Xin, H. Zhang and Q. Zhang, *Sensor. Actuat. B-Chem.*, 2014, **196**, 265-271.
203. J. Cao, X. Zhang, X. He, L. Chen and Y. Zhang, *Chem. Asian J.*, 2014, **9**, 526-533.
204. H. Chen, J. Kong, D. Yuan and G. Fu, *Biosens. Bioelectron.*, 2014, **53**, 5-11.
205. L. A. Peyser, A. E. Vinson, A. P. Bartko and R. M. Dickson, *Science*, 2001, **291**, 103-106.
206. J. T. Petty, J. Zheng, N. V. Hud and R. M. Dickson, *J. Am. Chem. Soc.*, 2004, **126**, 5207-5212.
207. P. D. Jadzinsky, G. Calero, C. J. Ackerson, D. A. Bushnell and R. D. Kornberg, *Science*, 2007, **318**, 430-433.
208. W. W. Guo, J. P. Yuan, Q. Z. Dong and E. K. Wang, *J. Am. Chem. Soc.*, 2010, **132**, 932-934.
209. L. Shang, S. J. Dong and G. U. Nienhaus, *Nano Today*, 2011, **6**, 401-418.
210. S. Choi, R. M. Dickson and J. H. Yu, *Chem. Soc. Rev.*, 2012, **41**, 1867-1891.
211. Y. Z. Lu and W. Chen, *Chem. Soc. Rev.*, 2012, **41**, 3594-3623.
212. Y. C. Shiang, C. C. Huang, W. Y. Chen, P. C. Chen and H. T. Chang, *J. Mater. Chem.*, 2012, **22**, 12972-12982.
213. J. Zheng, C. Zhou, M. X. Yu and J. B. Liu, *Nanoscale*, 2012, **4**, 4073-4083.
214. X. Yuan, Z. T. Luo, Y. Yu, Q. F. Yao and J. P. Xie, *Chem. Asian J.*, 2013, **8**, 858-871.
215. H. Kawasaki, K. Hamaguchi, I. Osaka and R. Arakawa, *Adv. Funct. Mater.*, 2011, **21**, 3508-3515.
216. L. Shang, F. Stockmar, N. Azadfar and G. U. Nienhaus, *Angew. Chem. Int. Ed.*, 2013, **52**, 11154-11157.

217. L. B. Zhang, J. B. Zhu, S. J. Guo, T. Li, J. Li and E. K. Wang, *J. Am. Chem. Soc.*, 2013, **135**, 2403-2406.
218. L. B. Zhang and E. K. Wang, *Nano Today*, 2014, **9**, 132-157.
219. J. F. Parker, C. A. Fields-Zinna and R. W. Murray, *Acc. Chem. Res.*, 2010, **43**, 1289-1296.
220. A. Desireddy, B. E. Conn, J. Guo, B. Yoon, R. N. Barnett, B. M. Monahan, K. Kirschbaum, W. P. Griffith, R. L. Whetten, U. Landman and T. P. Bigioni, *Nature*, 2013, **501**, 399-402.
221. H. Yang, Y. Wang, H. Huang, L. Gell, L. Lehtovaara, S. Malola, H. Häkkinen and N. Zheng, *Nat. Commun.*, 2013, **4**, 2422.
222. S. Antonello, G. Arrigoni, T. Dainese, M. De Nardi, G. Parisio, L. Perotti, A. Rene, A. Venzo and F. Maran, *ACS Nano*, 2014, **8**, 2788-2795.
223. T. Dainese, S. Antonello, J. A. Gascon, F. F. Pan, N. V. Perera, M. Ruzzi, A. Venzo, A. Zoleo, K. Rissanen and F. Maran, *ACS Nano*, 2014, **8**, 3904-3912.
224. L. Shang and S. Dong, *Chem. Commun.*, 2008, 1088-1090.
225. L. Shang and S. J. Dong, *J. Mater. Chem.*, 2008, **18**, 4636-4640.
226. L. Shang, R. M. Dorlich, S. Brandholt, R. Schneider, V. Trouillet, M. Bruns, D. Gerthsen and G. U. Nienhaus, *Nanoscale*, 2011, **3**, 2009-2014.
227. L. Shang, N. Azadfar, F. Stockmar, W. Send, V. Trouillet, M. Bruns, D. Gerthsen and G. U. Nienhaus, *Small*, 2011, **7**, 2614-2620.
228. L. Shang, S. Brandholt, F. Stockmar, V. Trouillet, M. Bruns and G. U. Nienhaus, *Small*, 2012, **8**, 661-665.
229. L. Shang and G. U. Nienhaus, *Biophys Rev.*, 2012, **4**, 313-322.
230. L. Shang and G. U. Nienhaus, *Mater. Today*, 2013, **16**, 58-66.
231. R. Jin, *Nanoscale*, 2010, **2**, 343-362.
232. G. Li, C. Zeng and R. Jin, *J. Am. Chem. Soc.*, 2014, **136**, 3673-3679.
233. Z. Luo, K. Zheng and J. Xie, *Chem. Commun.*, 2014, **50**, 5143-5155.
234. Y. Yu, Z. T. Luo, C. S. Teo, Y. N. Tan and J. P. Xie, *Chem. Commun.*, 2013, **49**, 9740-9742.
235. X.-D. Zhang, Z. Luo, J. Chen, X. Shen, S. Song, Y. Sun, S. Fan, F. Fan, D. T. Leong and J. Xie, *Adv. Mater.*, 2014, **26**, 4565-4568.
236. W. Wei, Y. Lu, W. Chen and S. Chen, *J. Am. Chem. Soc.*, 2011, **133**, 2060-2063.
237. M. Liu and W. Chen, *Nanoscale*, 2013, **5**, 12558-12564.
238. J. Sun, J. Zhang and Y. Jin, *J. Mater. Chem. C*, 2013, **1**, 138-143.
239. R. L. Whetten, M. N. Shafigullin, J. T. Khoury, T. G. Schaaff, I. Vezmar, M. M. Alvarez and A. Wilkinson, *Acc. Chem. Res.*, 1999, **32**, 397-406.
240. M. Walter, J. Akola, O. Lopez-Acevedo, P. D. Jadzinsky, G. Calero, C. J. Ackerson, R. L. Whetten, H. Grönbeck and H. Häkkinen, *Proc. Natl. Acad. Sci. USA*, 2008, **105**, 9157-9162.
241. Z. H. Qing, X. X. He, T. P. Qing, K. M. Wang, H. Shi, D. G. He, Z. Zou, L. Yan, F. Z. Xu, X. S. Ye and Z. G. Mao, *Anal. Chem.*, 2013, **85**, 12138-12143.
242. L. H. Jin, Y. X. Fang, L. Shang, Y. Q. Liu, J. Li, L. Wang, P. Hu and S. J. Dong, *Chem. Commun.*, 2013, **49**, 243-245.
243. L. Shang, L. X. Yang, F. Stockmar, R. Popescu, V. Trouillet, M. Bruns, D. Gerthsen and G. U. Nienhaus, *Nanoscale*, 2012, **4**, 4155-4160.
244. L. H. Jin, L. Shang, S. J. Guo, Y. X. Fang, D. Wen, L. Wang, J. Y. Yin and S. J. Dong, *Biosens. Bioelectron.*, 2011, **26**, 1965-1969.
245. L. Shang and S. J. Dong, *Biosens. Bioelectron.*, 2009, **24**, 1569-1573.
246. X. Yuan, B. Zhang, Z. T. Luo, Q. F. Yao, D. T. Leong, N. Yan and J. P. Xie, *Angew. Chem. Int. Ed.*, 2014, **53**, 4623-4627.
247. Q. F. Yao, Z. T. Luo, X. Yuan, Y. Yu, C. Zhang, J. P. Xie and J. Y. Lee, *Sci. Rep.*, 2014, **4**, 3848.
248. X. D. Zhang, J. Chen, Z. T. Luo, D. Wu, X. Shen, S. S. Song, Y. M. Sun, P. X. Liu, J. Zhao, S. D. Huo, S. J. Fan, F. Y. Fan, X. J. Liang and J. P. Xie, *Adv. Healthcare Mater.*, 2014, **3**, 133-141.
249. X. Yuan, M. I. Setyawati, A. S. Tan, C. N. Ong, D. T. Leong and J. P. Xie, *NPG Asia Mater.*, 2013, **5**, e39.
250. D. Y. Chen, Z. T. Luo, N. J. Li, J. Y. Lee, J. P. Xie and J. M. Lu, *Adv. Funct. Mater.*, 2013, **23**, 4324-4331.
251. Y. Yu, Q. F. Yao, Z. T. Luo, X. Yuan, J. Y. Lee and J. P. Xie, *Nanoscale*, 2013, **5**, 4606-4620.
252. X. Yuan, Y. Q. Tay, X. Y. Dou, Z. T. Luo, D. T. Leong and J. P. Xie, *Anal. Chem.*, 2013, **85**, 1913-1919.
253. C. J. Liu, J. Ling, X. Q. Zhang, J. Peng, Q. E. Cao and Z. T. Ding, *Anal. Methods*, 2013, **5**, 5584-5588.
254. A. Som, A. K. Samal, T. Udayabhaskararao, M. S. Bootharaju and T. Pradeep, *Chem. Mater.*, 2014, **26**, 3049-3056.
255. J. Hassinen, P. Pulkkinen, E. Kalenius, T. Pradeep, H. Tenhu, H. Hakkinen and R. H. A. Ras, *J. Phys. Chem. Lett.*, 2014, **5**, 585-589.
256. K. R. Krishnadas, T. Udayabhaskararao, S. Choudhury, N. Goswami, S. K. Pal and T. Pradeep, *Eur. J. Inorg. Chem.*, 2014, **2014**, 908-916.
257. A. Mathew, G. Natarajan, L. Lehtovaara, H. Hakkinen, R. M. Kumar, V. Subramanian, A. Jaleel and T. Pradeep, *ACS Nano*, 2014, **8**, 139-152.
258. I. Chakraborty, W. Kurashige, K. Kanehira, L. Gell, H. Hakkinen, Y. Negishi and T. Pradeep, *J. Phys. Chem. Lett.*, 2013, **4**, 3351-3355.
259. I. Chakraborty, S. Bag, U. Landman and T. Pradeep, *J. Phys. Chem. Lett.*, 2013, **4**, 2769-2773.
260. M. S. Bootharaju and T. Pradeep, *Langmuir*, 2013, **29**, 8125-8132.
261. S. Kumar, E. S. Shibu, T. Pradeep and A. K. Sood, *Opt. Express*, 2013, **21**, 8483-8492.
262. Y. Niihori, M. Matsuzaki, T. Pradeep and Y. Negishi, *J. Am. Chem. Soc.*, 2013, **135**, 4946-4949.
263. A. Ganguly, I. Chakraborty, T. Udayabhaskararao and T. Pradeep, *J. Nanopart. Res.*, 2013, **15**, 7.
264. K. S. Sugi, I. Chakraborty, T. Udayabhaskararao, J. S. Mohanty and T. Pradeep, *Part. Part. Syst. Charact.*, 2013, **30**, 241-243.
265. T. Udayabhaskararao, M. S. Bootharaju and T. Pradeep, *Nanoscale*, 2013, **5**, 9404-9411.
266. I. Chakraborty, T. Udayabhaskararao, G. K. Deepesh and T. Pradeep, *J. Mater. Chem. B*, 2013, **1**, 4059-4064.
267. M. S. Bootharaju, G. K. Deepesh, T. Udayabhaskararao and T. Pradeep, *J. Mater. Chem. A*, 2013, **1**, 611-620.
268. K. P. Remya, T. Udayabhaskararao and T. Pradeep, *J. Phys. Chem. C*, 2012, **116**, 26019-26026.
269. I. Chakraborty, A. Govindarajan, J. Erusappan, A. Ghosh, T. Pradeep, B. Yoon, R. L. Whetten and U. Landman, *Nano Lett.*, 2012, **12**, 5861-5866.
270. I. Chakraborty, T. Udayabhaskararao and T. Pradeep, *J. Hazard. Mater.*, 2012, **211**, 396-403.
271. A. George, E. S. Shibu, S. M. Maliyekkal, M. S. Bootharaju and T. Pradeep, *ACS Appl. Mater. Interfaces*, 2012, **4**, 639-644.
272. T. Udayabhaskararao, Y. Sun, N. Goswami, S. K. Pal, K. Balasubramanian and T. Pradeep, *Angew. Chem. Int. Ed.*, 2012, **51**, 2155-2159.
273. M. S. Bootharaju and T. Pradeep, *Langmuir*, 2011, **27**, 8134-8143.
274. E. S. Shibu and T. Pradeep, *Chem. Mater.*, 2011, **23**, 989-999.
275. M. A. H. Muhammed and T. Pradeep, *Small*, 2011, **7**, 204-208.
276. T. U. B. Rao, B. Nataraju and T. Pradeep, *J. Am. Chem. Soc.*, 2010, **132**, 16304-16307.
277. W. W. Guo, R. Orbach, I. Mironi-Harpaz, D. Seliktar and I. Willner, *Small*, 2013, **9**, 3748-3752.
278. R. Orbach, W. W. Guo, F. Wang, O. Lioubashevski and I. Willner, *Langmuir*, 2013, **29**, 13066-13071.
279. X. Q. Liu, F. Wang, A. Niazov-Elkan, W. W. Guo and I. Willner, *Nano Lett.*, 2013, **13**, 309-314.
280. J. Ai, W. W. Guo, B. L. Li, T. Li, D. Li and E. K. Wang, *Talanta*, 2012, **88**, 450-455.
281. W. W. Guo, J. P. Yuan and E. K. Wang, *Chem. Commun.*, 2012, **48**, 3076-3078.

282. J. P. Yuan, W. W. Guo and E. K. Wang, *Anal. Chim. Acta*, 2011, **706**, 338-342.
283. W. W. Guo, J. P. Yuan and E. K. Wang, *Chem. Commun.*, 2011, **47**, 10930-10932.
284. X. Yang, X. P. Sun, Z. Z. Lv, W. W. Guo, Y. Du and E. K. Wang, *Chem. Commun.*, 2010, **46**, 8818-8820.
285. W. W. Guo, J. P. Yuan and E. K. Wang, *Chem. Commun.*, 2009, 3395-3397.
286. S. Antonello, A. H. Holm, E. Instuli and F. Maran, *J. Am. Chem. Soc.*, 2007, **129**, 9836-9837.
287. S. Antonello, M. Hesari, F. Polo and F. Maran, *Nanoscale*, 2012, **4**, 5333-5342.
288. S. Antonello, N. V. Perera, M. Ruzzi, J. A. Gascon and F. Maran, *J. Am. Chem. Soc.*, 2013, **135**, 15585-15594.
289. S. Das, A. Goswami, M. Hesari, J. F. Al-Sharab, E. Mikmekova, F. Maran and T. Asefa, *Small*, 2014, **10**, 1473-1478.
290. M. A. H. Muhammed, P. K. Verma, S. K. Pal, A. Retnakumari, M. Koyakutty, S. Nair and T. Pradeep, *Chem. Eur. J.*, 2010, **16**, 10103-10112.
291. X. Le Guevel, B. Hotzer, G. Jung, K. Hollemeyer, V. Trouillet and M. Schneider, *J. Phys. Chem. C*, 2011, **115**, 10955-10963.
292. F. Wen, Y. H. Dong, L. Feng, S. Wang, S. C. Zhang and X. R. Zhang, *Anal. Chem.*, 2011, **83**, 1193-1196.
293. Y. C. Wang, Y. Wang, F. B. Zhou, P. Kim and Y. N. Xia, *Small*, 2012, **8**, 3769-3773.
294. J. S. Mohanty, P. L. Xavier, K. Chaudhari, M. S. Bootharaju, N. Goswami, S. K. Pal and T. Pradeep, *Nanoscale*, 2012, **4**, 4255-4262.
295. S. K. Sun, L. X. Dong, Y. Cao, H. R. Sun and X. P. Yan, *Anal. Chem.*, 2013, **85**, 8436-8441.
296. H. W. Li, Y. Yue, T. Y. Liu, D. M. Li and Y. Q. Wu, *J. Phys. Chem. C*, 2013, **117**, 16159-16165.
297. J. M. Liu, J. T. Chen and X. P. Yan, *Anal. Chem.*, 2013, **85**, 3238-3245.
298. S. Ghosh, U. Anand and S. Mukherjee, *Anal. Chem.*, 2014, **86**, 3188-3194.
299. R. Ghosh, A. K. Sahoo, S. S. Ghosh, A. Paul and A. Chattopadhyay, *ACS Appl. Mater. Interfaces*, 2014, **6**, 3822-3828.
300. N. Goswami, A. Baksi, A. Giri, P. L. Xavier, G. Basu, T. Pradeep and S. K. Pal, *Nanoscale*, 2014, **6**, 1848-1854.
301. Y. L. Liu, K. L. Ai, X. L. Cheng, L. H. Huo and L. H. Lu, *Adv. Funct. Mater.*, 2010, **20**, 951-956.
302. N. Goswami, A. Giri, M. S. Bootharaju, P. L. Xavier, T. Pradeep and S. K. Pal, *Anal. Chem.*, 2011, **83**, 9676-9680.
303. K. Choudhari, P. L. Xavier and T. Pradeep, *J. Biomed. Nanotechnol.*, 2011, **7**, 70-71.
304. A. H. Holm, M. Ceccato, R. L. Donkers, L. Fabris, G. Pace and F. Maran, *Langmuir*, 2006, **22**, 10584-10589.
305. W. Y. Chen, J. Y. Lin, W. J. Chen, L. Y. Luo, E. W. G. Diau and Y. C. Chen, *Nanomedicine*, 2010, **5**, 755-764.
306. Y. H. Lin and W. L. Tseng, *Anal. Chem.*, 2010, **82**, 9194-9200.
307. H. Kong, Y. X. Lu, H. Wang, F. Wen, S. C. Zhang and X. R. Zhang, *Anal. Chem.*, 2012, **84**, 4258-4261.
308. Y. Tao, Y. H. Lin, Z. Z. Huang, J. S. Ren and X. G. Qu, *Adv. Mater.*, 2013, **25**, 2594-2599.
309. A. Baksi, P. L. Xavier, K. Chaudhari, N. Goswami, S. K. Pal and T. Pradeep, *Nanoscale*, 2013, **5**, 2009-2016.
310. Y. Xu, J. Sherwood, Y. Qin, D. Crowley, M. Bonizzoni and Y. Bao, *Nanoscale*, 2014, **6**, 1515-1524.
311. A. Baksi, T. Pradeep, B. Yoon, C. Yannouleas and U. Landman, *Chemphyschem*, 2013, **14**, 1272-1282.
312. D. Lu, L. Liu, F. Li, S. Shuang, Y. Li, M. M. F. Choic and C. Dong, *Spectrochim. Acta A* 2014, **121**, 77-80.
313. C.-J. Yu, T.-H. Chen, J.-Y. Jiang and W.-L. Tseng, *Nanoscale*, 2014, **6**, 9618-9624.
314. P. H. Chan, S. Y. Wong, S. H. Lin and Y. C. Chen, *Rapid Commun. Mass Sp.*, 2013, **27**, 2143-2148.
315. T. H. Chen, C. Y. Lu and W. L. Tseng, *Talanta*, 2013, **117**, 258-262.
316. A. Baksi and T. Pradeep, *Nanoscale*, 2013, **5**, 12245-12254.
317. S. S. Narayanan and S. K. Pal, *J. Phys. Chem. C*, 2008, **112**, 4874-4879.
318. T. Ueno, T. Koshiyama, T. Tsuruga, T. Goto, S. Kanamaru, F. Arisaka and Y. Watanabe, *Angew. Chem. Int. Ed.*, 2006, **45**, 4508-4512.
319. M. Knez, A. M. Bittner, F. Boes, C. Wege, H. Jeske, E. Maiβ and K. Kern, *Nano Lett.*, 2003, **3**, 1079-1082.
320. L. Rastogi and J. Arunachalam, *Colloid. Surface. B.*, 2013, **108**, 134-141.
321. S. Gautam, P. Dubey and M. N. Gupta, *Colloid. Surface. B.*, 2013, **102**, 879-883.
322. M. S. Bakshi, H. Kaur, T. S. Banipal, N. Singh and G. Kaur, *Langmuir*, 2010, **26**, 13535-13544.
323. G. Wei, F. Xu, Z. Li and K. D. Jandt, *J. Phys. Chem. C*, 2011, **115**, 11453-11460.
324. T. Yang, Y. Zhang and Z. Li, *Biomacromolecules*, 2011, **12**, 2027-2031.
325. Y. Lee and K. E. Geckeler, *J. Biomed. Mater. Res. A*, 2012, **100A**, 848-855.
326. R. Das, R. Jagannathan, C. Sharan, U. Kumar and P. Poddar, *J. Phys. Chem. C*, 2009, **113**, 21493-21500.
327. H. Cai and P. Yao, *Nanoscale*, 2013, **5**, 2892-2900.
328. D. M. Eby, N. M. Schaeublin, K. E. Farrington, S. M. Hussain and G. R. Johnson, *ACS Nano*, 2009, **3**, 984-994.
329. M. Fujiwara, K. Shiokawa, M. Araki, N. Ashitaka, K. Morigaki, T. Kubota and Y. Nakahara, *Cryst. Growth Des.*, 2010, **10**, 4030-4037.
330. X. Q. Wang, H. L. Sun, Y. Q. Xia, C. X. Chen, H. Xu, H. H. Shan and J. R. Lu, *J. Colloid Interf. Sci.*, 2009, **332**, 96-103.
331. A. E. Voinescu, D. Touraud, A. Lecker, A. Pfitzner, W. Kunz and B. W. Ninham, *Langmuir*, 2007, **23**, 12269-12274.
332. K. Zhao, M. Wang, X. Q. Wang, C. M. Wu, H. Xu and J. R. Lu, *Cryst. Growth Des.*, 2013, **13**, 1583-1589.
333. C. Jimenez-Lopez, A. Rodriguez-Navarro, J. M. Dominguez-Vera and J. M. Garcia-Ruiz, *Geochim. Cosmochim. Acta*, 2003, **67**, 1667-1676.
334. M. B. Cardoso, H. R. Luckarift, V. S. Urban, H. O'Neill and G. R. Johnson, *Adv. Funct. Mater.*, 2010, **20**, 3031-3038.
335. Y. Jiang, D. Yang, L. Zhang, Y. Jiang, Y. Zhang, J. Li and Z. Jiang, *Ind. Eng. Chem. Res.*, 2008, **47**, 1876-1882.
336. L. Zhang, D. Z. Qin, Q. R. Liu and G. X. He, *Micro Nano Lett.*, 2012, **7**, 115-117.
337. D. Z. Qin, L. Zhang, G. X. He and Q. R. Liu, *Mater. Lett.*, 2012, **66**, 7-9.
338. L. Zhang, G. R. Yang, G. X. He, L. Wang, Q. R. Liu, Q. X. Zhang and D. Z. Qin, *Appl. Surf. Sci.*, 2012, **258**, 8185-8191.
339. L. N. Hassani, F. Hindre, T. Beuvier, B. Calvignac, N. Lautram, A. Gibaud and F. Boury, *J. Mater. Chem. B*, 2013, **1**, 4011-4019.
340. X. He, L. Gao and N. Ma, *Sci. Rep.*, 2013, **3**, 2825.
341. H. Wei and E. Wang, *Chem. Lett.*, 2007, **36**, 210-211.
342. H. Wei, J. Liu, L. Zhou, J. Li, X. Jiang, J. Kang, X. Yang, S. Dong and E. Wang, *Chem. Eur. J.*, 2008, **14**, 3687-3693.
343. H. Wei, L. L. Zhou, J. Li, J. F. Liu and E. K. Wang, *J. Colloid Interf. Sci.*, 2008, **321**, 310-314.
344. D. Ivnitski, K. Artyushkova, R. A. Rincón, P. Atanassov, H. R. Luckarift and G. R. Johnson, *Small*, 2008, **4**, 357-364.
345. T. M. Garakani, H. Wang, T. Krappitz, B. M. Liebeck, P. van Rijn and A. Boker, *Chem. Commun.*, 2012, **48**, 10210-10212.
346. T. Shiomi, T. Tsunoda, A. Kawai, F. Mizukami and K. Sakaguchi, *Chem. Commun.*, 2007, 4404-4406.
347. T. Shiomi, T. Tsunoda, A. Kawai, H. Chiku, F. Mizukami and K. Sakaguchi, *Chem. Commun.*, 2005, 5325-5327.
348. F. Gao, Q. Lu and S. Komarneni, *Chem. Commun.*, 2005, 531-533.
349. Y. Takeda, T. Kondow and F. Mafune, *Chem. Phys. Lett.*, 2011, **504**, 175-179.
350. T. Koshiyama, N. Kawaba, T. Hikage, M. Shirai, Y. Miura, C. Y. Huang, K. Tanaka, Y. Watanabe and T. Ueno, *Bioconjugate Chem.*, 2010, **21**, 264-269.
351. M. Liang, L. B. Wang, R. X. Su, W. Qi, M. F. Wang, Y. J. Yu and Z. M. He, *Catal. Sci. Technol.*, 2013, **3**, 1910-1914.

352. M. Liang, L. B. Wang, X. Liu, W. Qi, R. X. Su, R. L. Huang, Y. J. Yu and Z. M. He, *Nanotechnology*, 2013, **24**, 245601.
353. P. G. Vekilov, *Nat. Nanotechnol.*, 2011, **6**, 82-83.
354. O. L. Muskens, M. W. England, L. Danos, M. Li and S. Mann, *Adv. Funct. Mater.*, 2013, **23**, 281-290.
355. Y. Takeda and F. Mafune, *Chem. Phys. Lett.*, 2014, **604**, 110-115.
356. H. Tabe, S. Abe, T. Hikage, S. Kitagawa and T. Ueno, *Chem. Asian J.*, 2014, **9**, 1373-1378.
357. T. Koshiyama, M. Shirai, T. Hikage, H. Tabe, K. Tanaka, S. Kitagawa and T. Ueno, *Angew. Chem. Int. Ed.*, 2011, **50**, 4849-4852.
358. N. Yokoi, H. Inaba, M. Terauchi, A. Z. Stieg, N. J. M. Sanghamitra, T. Koshiyama, K. Yutani, S. Kanamaru, F. Arisaka, T. Hikage, A. Suzuki, T. Yamane, J. K. Gimzewski, Y. Watanabe, S. Kitagawa and T. Ueno, *Small*, 2010, **6**, 1873-1879.
359. T. Ueno, H. Tabe and Y. Tanaka, *Chem. Asian J.*, 2013, **8**, 1646-1660.
360. T. Ueno, M. Abe, K. Hirata, S. Abe, M. Suzuki, N. Shimizu, M. Yamamoto, M. Takata and Y. Watanabe, *J. Am. Chem. Soc.*, 2009, **131**, 5094-5100.
361. B. Wang, C. L. Guo, G. J. Chen, B. Park and B. Q. Xu, *Chem. Commun.*, 2012, **48**, 1644-1646.
362. C. L. Guo, B. Wang, L. C. Wang and B. Q. Xu, *Chem. Commun.*, 2012, **48**, 12222-12224.
363. M. J. Han, H. Yun and S. Y. Lee, *Biotechnol. Adv.*, 2008, **26**, 591-609.
364. A. Y. Chen, Z. T. Deng, A. N. Billings, U. O. S. Seker, M. Y. Lu, R. J. Citorik, B. Zakeri and T. K. Lu, *Nat. Mater.*, 2014, **13**, 515-523.
365. M. V. Cespedes, U. Unzueta, W. Tatkiewicz, A. Sanchez-Chardi, O. Conchillo-Sole, P. Alamo, Z. K. Xu, I. Casanova, J. L. Corchero, M. Pesarrodona, J. Cedano, X. Daura, I. Ratera, J. Veciana, N. Ferrer-Miralles, E. Vazquez, A. Villaverde and R. Mangues, *ACS Nano*, 2014, **8**, 4166-4176.
366. J. Grzyb, *Acta Phys. Pol. A*, 2012, **122**, 279-283.

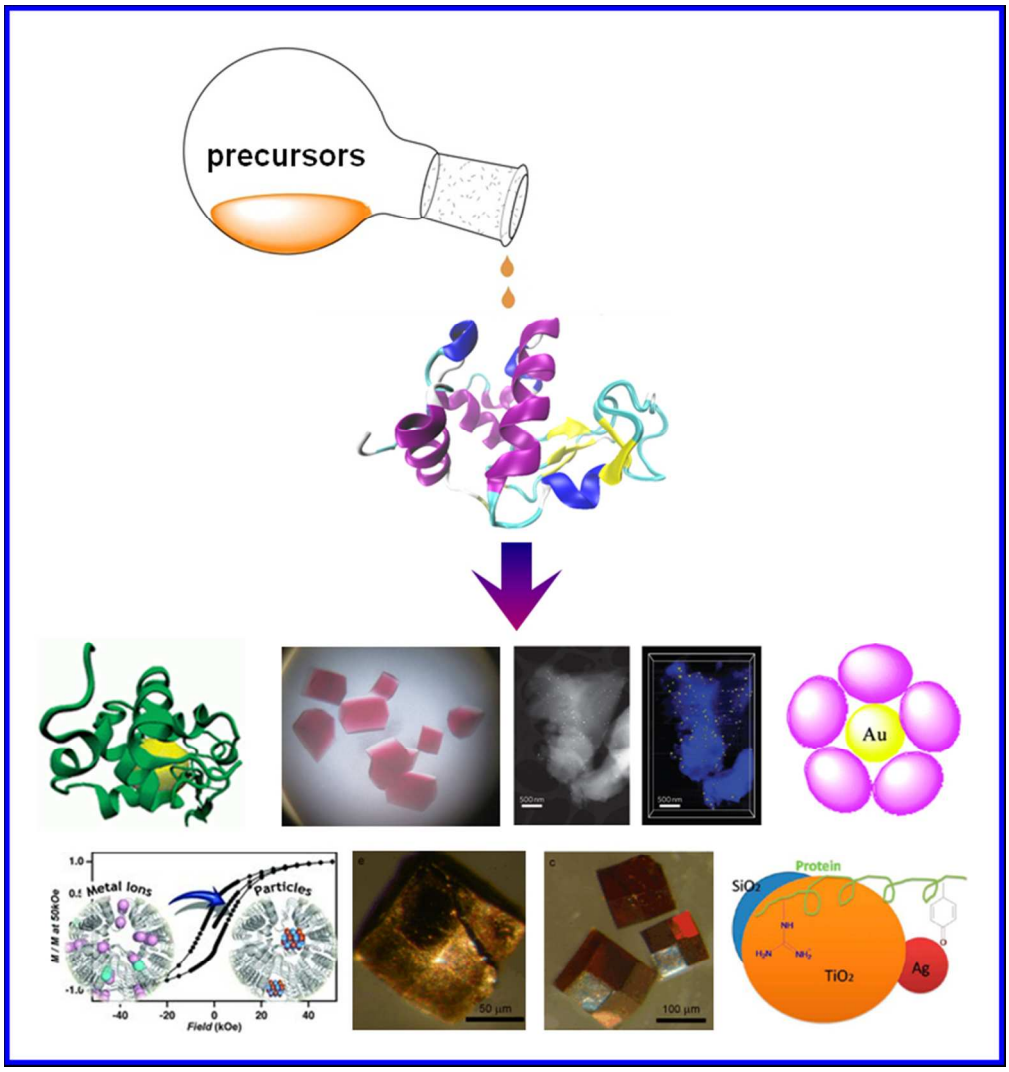

139x147mm (150 x 150 DPI)

Using lysozyme as a model, protein-directed approaches to functional nanomaterials have been reviewed, making rational materials design possible in future.